Molecular Therapy
Original Article

Glycogen Reduction in Myotubes of Late-Onset Pompe Disease Patients Using Antisense Technology

Elisa Goina,[1] Paolo Peruzzo,[2] Bruno Bembi,[2] Andrea Dardis,[2] and Emanuele Buratti[1]

[1]International Centre for Genetic Engineering and Biotechnology, Area Science Park, Padriciano, 34149 Trieste, Italy; [2]Regional Coordinator Centre for Rare Diseases, Academic Hospital Santa Maria della Misericordia, 33100 Udine, Italy

Glycogen storage disease type II (GSDII) is a lysosomal disorder caused by the deficient activity of acid alpha-glucosidase (GAA) enzyme, leading to the accumulation of glycogen within the lysosomes. The disease has been classified in infantile and late-onset forms. Most late-onset patients share a splicing mutation c.-32-13T > G in intron 1 of the *GAA* gene that prevents efficient recognition of exon 2 by the spliceosome. In this study, we have mapped the splicing silencers of *GAA* exon 2 and developed antisense morpholino oligonucleotides (AMOs) to inhibit those regions and rescue normal splicing in the presence of the c.-32-13T > G mutation. Using a minigene approach and patient fibroblasts, we successfully increased inclusion of exon 2 in the mRNA and GAA enzyme production by targeting a specific silencer with a combination of AMOs. Most importantly, the use of these AMOs in patient myotubes results in a decreased accumulation of glycogen. To our knowledge, this is the only therapeutic approach resulting in a decrease of glycogen accumulation in patient tissues beside enzyme replacement therapy (ERT) and TFEB overexpression. As a result, it may represent a highly novel and promising therapeutic line for GSDII.

INTRODUCTION

Glycogen storage disease type II (GSDII [OMIM: 232300], or Pompe disease), is an autosomal recessive lysosomal storage disorder caused by the deficient activity of acid alpha-glucosidase (GAA), an enzyme responsible for the degradation of glycogen within the lysosomes. The resulting glycogen accumulation causes swelling of the lysosomes, cellular dysfunction, and defective autophagy in numerous tissues, but cardiac and skeletal muscles are primarily involved.[1] Clinically, GSDII is characterized by a highly variable phenotype ranging from a rapidly progressive infantile-onset (IO) form to a slowly progressive late-onset (LO) form.[2] The classic IO phenotype manifests soon after birth and is characterized by absent or nearly absent enzyme activity, severe muscle weakness, cardiomegaly or cardiomyopathy, and respiratory insufficiency that typically lead to death within the first year of life.[3,4] The LO phenotype, manifests later in childhood, adolescence, or adulthood.[5] Patients retain some residual GAA enzyme activity (from 1% to 30%), and display a less severe and slow progressive disease characterized by skeletal muscle weakness, without cardiac involvement, and respiratory complications, resulting in severe physical handicap that heavily affects the quality of life.[6,7]

The only approved specific treatment for GSDII is enzyme replacement therapy (ERT) using recombinant human GAA (rhGAA). It has been clearly demonstrated that ERT improves cardiac function, motor skills, and lifespan in patients affected by the IO phenotype.[8,9] However, it leads to mild and variably improvements in motor and respiratory function in LO patients.[10,11] Thus, innovative and more effective therapies are needed.

The *GAA* gene (OMIM: 606800, Ensembl Gene ID ENSG00000171298) maps to human chromosome 17q25.2-25.3 and contains 20 exons. The first exon is not translated, and it is separated by a large intron from exon 2, where the ATG start codon is located (Ensembl Transcript ID ENST00000302262.7). Its cDNA encodes for a protein of 952 amino acids. The enzyme is synthesized as a catalytically inactive 110-kDa precursor that undergoes post-translational glycosylation and proteolytic processing, resulting in 76-kDa and 70-kDa mature enzymes active within lysosomes.[12]

To date, 497 mutations in the *GAA* gene have been identified (http://www.hgmd.cf.ac.uk), including missense, nonsense, splice-site mutations, and small and large intragenic deletions and insertions.[13,14] Few pathogenic mutations occur with high frequency in different ethnic groups (p.R854X among African Americans, p.D645E among Asians, and del525T among Dutch people). However, most mutations are present in individuals or a small number of families.[15–17] The only exception is represented by the intronic mutation c.-32-13T > G that is present in 40%–70% of the alleles in patients affected with the LO form of GSDII.[6,18–22]

Received 9 February 2017; accepted 25 May 2017;
http://dx.doi.org/10.1016/j.ymthe.2017.05.019.

Correspondence: Emanuele Buratti, ICGEB, Padriciano 99, 34149 Trieste, Italy.
E-mail: buratti@icgeb.org
Correspondence: Andrea Dardis, Regional Coordinator Centre for Rare Diseases, Academic Hospital Santa Maria della Misericordia, Piazzale Santa Maria della Misericordia 15, 33100 Udine, Italy.
E-mail: andrea.dardis@asuiud.sanita.fvg.it

In a previous study, we have shown that this mutation abrogates the binding of the splicing factor U2AF65 to the polypyrimidine tract of exon 2, affecting the general efficiency of the splicing process that, in turn, leads to the complete or partial exclusion of exon 2 from the mRNA, splicing variants SV2 and SV3, respectively. However, it does not prevent the expression of the normal spliced transcript (N) and the synthesis of an enzymatically active GAA protein.[23,24] Therefore, patients carrying the c.-32-13T > G mutation display variable levels of GAA residual activity that would be enough to delay the phenotypic expression of the disease.[25,26]

Until recently, strategies aimed at rescuing the normal splicing of transcripts carrying this mutation had not been explored. However, the possibility to restore or increase normal splicing of the *GAA* exon 2 of transcripts carrying the c.-32-13T > G mutation is particularly appealing considering that (1) almost all LO patients carry this mutation in at least one allele and (2) some patients express up to 30% of normal GAA activity and just a little increase in exon inclusion might be enough to achieve a beneficial effect in clinical settings.[14,27]

Recently, we provided in vitro evidence clearly showing that it is possible to modulate the expression of normal spliced GAA mRNA of c.-32-13T > G mutated (MUT) alleles, both by overexpressing mRNA binding proteins and by using small molecules.[26] Several strategies have been developed to rescue or increase normal splicing of transcripts carrying mutations that affect the splicing process. Among them, the use of antisense oligonucleotide technology represents a promising approach.[28,29] In this work, we have identified several silencer elements in the exon 2 of *GAA* pre-mRNA and described the feasibility of splicing correction using antisense oligonucleotides as a personalized therapy for LO-GSDII patients.

RESULTS

Identification of Splicing Regulatory Elements within GAA Exon 2

We have previously demonstrated that the c.-32-13T > G mutation affects the overall splicing efficiency of *GAA* exon 2, leading to its partial or total exclusion from the mature transcript, mainly by abrogating U2AF65 binding to the pre-mRNA.[26] However, considering that the mutation occurs outside the acceptor site of the unusually long exon 2 (578 nt), it is likely that several splicing regulatory elements are involved in the regulation of exon 2 splicing efficiency. In keeping with this view, the overexpression of different splicing factors partially rescue *GAA* exon 2 inclusion in the presence of the c.-32-13T > G *GAA* mutation.[26]

To verify this hypothesis, we looked for putative regulatory splicing elements located within this exon by creating a series of seven overlapping deletion constructs (140 nt), using as a template a previously described minigene containing the sequence of wild-type (WT) or c.-32-13T > G MUT *GAA* exon 2 (Figure 1A).[26] Initially, these constructs were transiently transfected in HeLa cells, and the splicing variants originated were analyzed by RT-PCR.

As shown in Figure 1B, the Δ147–286 and Δ357–500 deletions of exon 2 resulted in 23% and 35% increases of exon inclusion when compared with the full-length MUT minigene (Figure 1B, lanes 5 and 8; Figure S1A). This strongly suggested the presence of silencer elements located within these regions. Conversely, the Δ427–572 deletion resulted in the complete skipping of the exon 2 (Figure 1B, lane 9), indicating that this sequence acted as an enhancer element.

In addition to the mRNA variants resulting from the complete inclusion and total exclusion of exon 2, an extra variant was detected in cells transfected with the Δ357–500 construct (Figure 1B, lane 8). Sequencing analysis of this variant showed that the extra band results from the activation of a new cryptic 3 primt splice site (3′ss) (c3), 90 nt upstream of the deletion (Figure S1C).

In parallel to this analysis, the same deletions were created in the context of the WT minigene. As shown in Figure 1C, the effects of exon 2 deletions on the splicing pattern were similar to those observed in the MUT context. The Δ147–286 and Δ357–500 of exon 2 resulted in 90% and 88% increases of exon inclusion (Figure 1C, lanes 5 and 8; Figure S1B), while the exonic Δ427–572 resulted in complete exon 2 skipping (Figure 1C, lane 9). This result showed that these silencer and enhancer regions also play a role in regulating splicing of the WT exon and are not strictly related to the presence or absence of the c.-32-13 T > G mutation.

Identification of Splicing Factors Able to Bind *GAA* Exon 2 Regulatory Regions

To identify the specific *trans*-acting factors binding to these regulatory sequences, we performed RNA pull-down analysis. The pull-down experiment was carried out using three in vitro transcribed RNAs corresponding to the 140 nt sequence deleted in each construct that showed an effect on GAA exon 2 splicing: 147–286, 357–500, and 427–572 (Figure 2A). Using this approach, we identified five proteins selectively precipitated by each RNA and analyzed them by mass spectrometry (Figure 2B). The doublet band of an apparent molecular weight of 32–35 kDa (Figure 2B, letters a and b) corresponded to hnRNPA1 and its close homolog hnRNPA2 splicing factor. The sequence of the ∼50-kDa band (Figure 2B, letter c) matched with the hnRNPH protein. Finally, the two bands of ∼60 and 75 kDa (Figure 2B, letters d and e) were identified as hnRNPQ and hnRNPR factors, respectively. These results are largely consistent with expected outcomes when looking at splicing silencer elements.

The protein identity obtained by mass spectrometry analysis was confirmed by pull-down followed by western blot analysis using specific antibodies. As shown in Figure 2C, hnRNPA1 and hnRNPA2 bind the 147–287 region, hnRNPH recognizes the 357–500 sequence, and hnRNPQ and R preferentially bind the 427–572 region of GAA exon 2.

Although hnRNPs are the most abundant proteins within the nucleus, it is likely that other proteins could bind GAA exon 2 regulatory

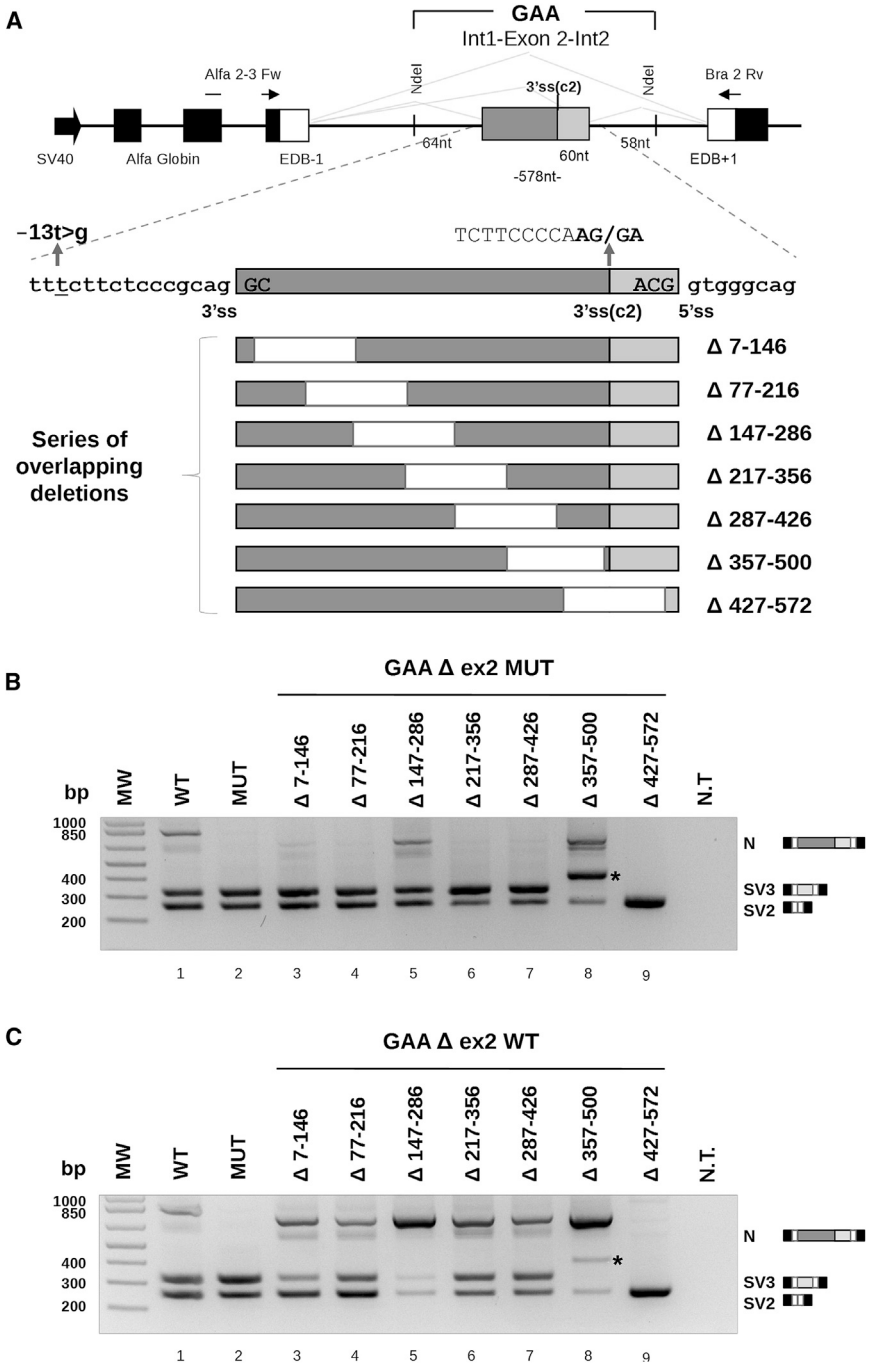

Figure 1. Splicing Effect of Serial Deletions Performed on MUT and WT *GAA* Exon 2 Minigenes

(A) Schematic illustration of the human *GAA* hybrid minigene and exonic deletions. The central part contains exon 2, part of intron 1, and part of intron 2 of the *GAA* gene. The Alfa Globin, fibronectin extra domain-B (EDB), and human *GAA* exons are shown as black, white, and gray boxes, respectively. The light gray box of *GAA* exon 2 represents the 60 nt included in the activation of the cryptic 3′ss (c2). Specific primers for RT-PCR analysis are represented by black arrows. The T-to-G substitution at position −13 of intron 1 (c.-32-13T > G) is in bold. Deletions of 140 nt within *GAA* exon 2 MUT and WT sequences are indicated by white boxes, and nucleotide numbers positions are reported in the lower part of the figure. (B and C) RT-PCR analysis of serial deletion of exon 2 on the MUT (B) and WT (C) minigene after HeLa transient transfection. Three resulting splicing variants corresponding to *GAA* exon 2 inclusion (N), exclusion (SV2), and 3′ss cryptic activation (SV3) are expressed by the WT construct, while the MUT minigene produced only the SV2 and SV3 variants. The agarose gel pictures show a representative result of three independent experiments. Not transfected (NT) cells were used as RT-PCR control. The asterisks indicate a splicing variant resulting from the activation of a new cryptic 3′ss (c3) in both MUT and WT Δ357–500 constructs.

sequences. As reported in our previous study,[26] SR splicing factors (SRSFs) are also involved in *GAA* exon 2 splicing regulation, with SRSF4 (SRp75) as the most effective in promoting exon inclusion.

Therefore, we decided to perform a new pull-down experiment, followed by western blot, searching specifically for SRSFs (Figure S2A). The obtained results showed that SRSF4, SRSF6 (SRp55), and SRSF5 (SRp40) bind the 427–572 sequence. SRSF4 and SRSF6 also bind the 147–286 region, though to a lesser extent. SRSF9 binds the 147–286 sequence, while none of the tested SRSFs bind the 357–500 sequence (Figure S2A).

SpliceAid 2,[30] an in silico splicing factor binding prediction tool, showed the presence of several hnRNPA1 and hnRNPH binding sites within the 147–286 and 357–500 sequences (Figures S2B and S2C), perfectly matching the pull-down and overexpression results.[26] In addition, in agreement with our western blot results (Figure S2A), the region between 427 and 572 nt of exon 2 was predicted to bind SRSF6 and SRSF5 (Figure S2D). Because numerous other algorithms predict splicing regulatory elements, we also analyzed our GAA exon 2 silencer and enhancer sequences using the Human Splicing Finder 3 (HSF3) program[31] (Figure S3). HSF3 integrates all available matrices to identify exonic motifs summarizing the analysis in an enhancer/silencer ratio curve. The analysis of the 147–286 nt sequence didn't show the presence of a strong silencer but suggested that the first part of the sequence contains an enhancer element (Figure S3A). In the case of 357–500 nt, two enhancers and a silencer regions were suggested to be present (Figure S3B). Finally, for 427–572 nt of exon 2, a strong enhancer sequence was highlighted in the first part of the region and a minor enhancer and a silencer were predicted (Figure S3C).

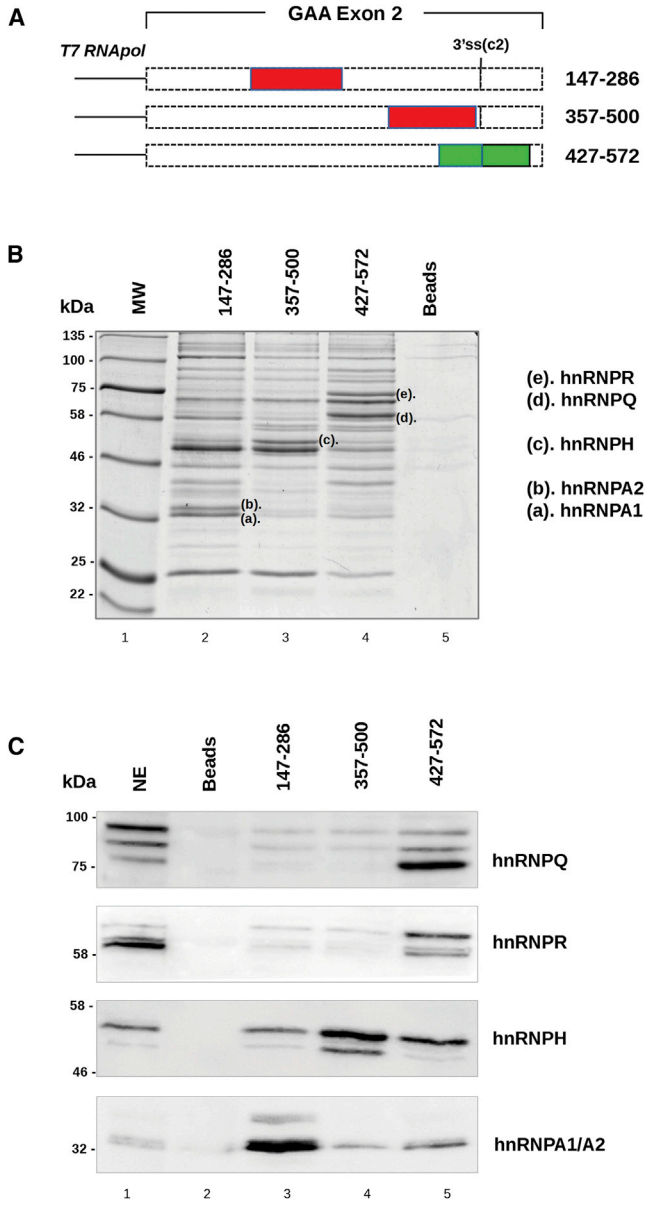

Figure 2. Identification of Proteins Able to Bind *GAA* Exon 2 by Pull-Down and Western Blot Analysis

(A) Schematic representation of *GAA* 147–286, 357–500, and 427–572 exonic regions used as templates for T7 RNA transcription in vitro. Putative silencers are represented by red boxes, while the putative enhancer is in green. (B) Pull-down analysis of three in vitro transcribed RNAs with HeLa nuclear extract (NE) analyzed on SDS-10% polyacrylamide gels and visualized by colloidal Coomassie staining. Proteins differentially precipitated by each RNA (letters a–e) were excised from the gel and analyzed by mass spectrometry. Colloidal Coomassie gel staining gives a representative picture of three independent experiments. Beads alone were used as a control (Beads). (C) Western blot analysis, after pull-down assay, using specific antibodies against hnRNPA1/A2, hnRNPH, hnRNPQ, and hnRNPR confirmed the identity of each protein. The nuclear extract sample corresponds to 1/20th of the total amount of protein used for the pull-down assay. The western blot images are representative pictures of three independent experiments. Beads alone were used as a control.

In conclusion, both programs agree that the identified regions can bind numerous splicing regulatory factors.

Correction of Exon 2 Skipping by AMOs in *GAA* MUT Minigene

Antisense morpholino oligonucleotides (AMOs) have been widely used to modulate splice-site utilization in pre-mRNAs splicing and in particular to target inhibitory sequences by blocking the binding of negative splicing factors and/or secondary structures formation.[32] Therefore, to block the effect of *GAA* exon 2 silencer elements in vivo, it was decided to use AMOs against the two identified regions (147–286 and 357–500 nt).

As a result, different AMOs directed against these regions were designed, taking into consideration the guanine-cytosine (GC) content, self-dimerization, nucleic acid melting temperature values, and putative binding sites for hnRNPA1/A2 and hnRNPH identified in the pull-down analysis. Three AMOs (1, 2, and 3) targeting the 147–286 exon 2 region (Figure 3A) were tested in different combinations (as single units, in couples, and all three) in HeLa cells co-transfected with the GAA MUT minigene. AMO 1 alone or combined with AMOs 2 or 3 and AMOs 1, 2, and 3 significantly promoted exon inclusion, while AMOs 2 and 3, alone or combined, had no effect on GAA exon 2 splicing (Figure 3B). However, the combination of AMO 1+2+3 was the most effective, leading to a 2.5-fold increase of exon 2 inclusion (Figure 3C). A standard AMO, fluorescently labeled, was used as a control for transfection (Figure S4). Its delivery, together with the GAA MUT minigene, did not affect the splicing pattern of the minigene itself, supporting the specificity of the AMO 1+2+3 effect (Figure S4A). Then, we investigated the possibility of using AMOs to promote GAA exon 2 inclusion by targeting the other putative silencer element, the 357–500 nt exon 2 sequence. Three AMOs (5, 6, and 7) were designed against this region (Figure S5A) and were tested in different combinations (as single units, in couples and all three). In particular, AMOs 5 and 7 alone and combined were able to slightly promote GAA exon 2 inclusion, while the combination of AMO 5+6+7 shifted the GAA splicing toward exon 2 inclusion, leading to about 2-fold of increase compared with the control (Figures S5B and S5C).

Correction of *GAA* Exon 2 Skipping by AMOs in Patient Fibroblasts Carrying the c.-32-13T > G Mutation

Because of their greater efficiency in rescuing exon 2 splicing, we decided to test the effect of AMOs 1, 2, and 3 on cultured fibroblasts obtained from a patient carrying the c.-32-13T > G mutation in heterozygosis with an unknown mutation that abrogated the expression of the other allele.[18] This cellular model is particularly useful, because every potential effect of AMO therapy would be solely attributable to the correction of the splicing defect due to the c.-32-13T > G mutation. Under basal conditions, the fibroblast from in this patient retained 20% of enzymatic activity when compared with WT cells (Figure S6A). As shown in Figure 4A, the treatment of fibroblasts with the combination of AMOs 1, 2, and 3 resulted in successful rescue of normally spliced *GAA* mRNA. As in the minigene system, AMO

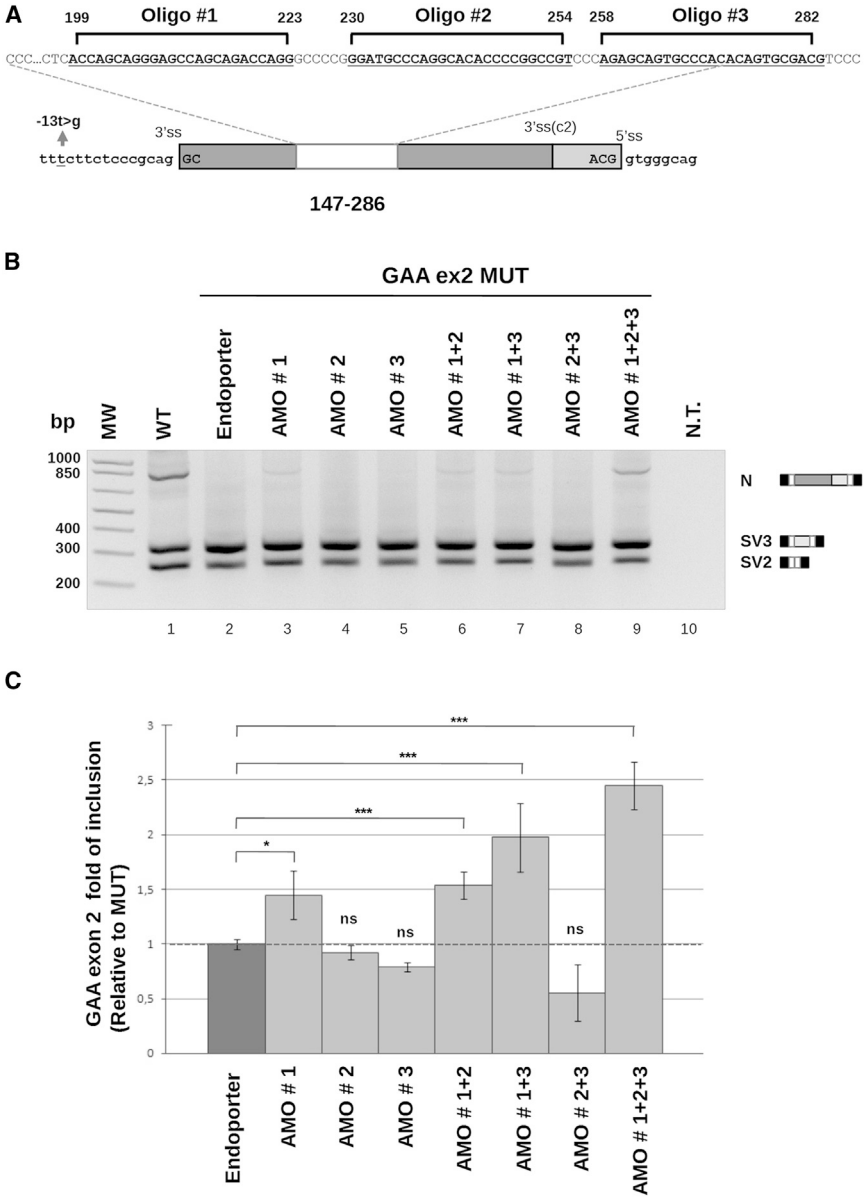

Figure 3. Effect of AMOs against Region 147–286 on Exon 2 Inclusion in the MUT Minigene Context

(A) Schematic representation of AMOs 1, 2, and 3 targeting the 147–286 region of *GAA* exon 2. The AMOs' target sequences are indicated by black lines. (B) RT-PCR analysis of HeLa cells co-transfected with AMOs 1, 2, and 3 and the *GAA* MUT minigene. AMOs were delivered as a single unit or in different combinations to a final concentration of 15 μM. Cells transfected with the mutated minigene, together with Endo-Porter reagent, were used as internal control; not transfected (NT) cells were used as RT-PCR control. The agarose gel picture shows a representative result of three independent experiments. (C) qRT-PCR analysis of *GAA* exon 2 inclusion (N) in cells co-transfected with AMOs (1, 2, and 3) and the *GAA* MUT minigene alone. The absolute abundance of the N form is normalized on AlfaGlobin expressed as the fold of increase over the minigene alone. qRT-PCR data are represented as mean ± SEM of three independent experiments in a histogram plot (*$p < 0.05$, ***$p < 0.001$).

1 alone was also partially effective in correcting the splicing profile of GAA mRNA (Figure 4A).

Real-time qPCR using primers that specifically amplify the normal *GAA* mRNA variant confirmed a 2.5-fold increase in the total amount of normal spliced *GAA* mRNA in fibroblasts treated with AMOs 1, 2, and 3 compared to mock-treated fibroblasts (Figure 4B). As a consequence of this increase, in treated fibroblasts, about 30% of total GAA mRNA was represented by the normal spliced GAA mRNA (Figure S7A). More importantly, the effect of the AMO combined treatment on normal spliced *GAA* mRNA was associated with an increase in GAA protein level (Figure 4C) and a 50% increase in GAA enzymatic activity (Figure 4D).

Reduction of Glycogen Accumulation in Myotubes from GAA Patients that Carry the c.-32-13T > G Mutation

As a consequence of the loss in GAA expression, the pivotal detrimental characteristic of LO-GSDII is the accumulation of glycogen within the lysosomes of skeletal muscle cells. Therefore, to assess the potential effects of AMO treatment on *GAA* normal spliced mRNA expression and activity, as well as on the pathological phenotype in muscle cells, we obtained myoblasts from a LO-GSDII patient who presented the c.-32-13T > G mutation in compound heterozygosity with the c.2646_2646+1delTG mutation in exon 18. This latter mutation was already known to cause the abrogation of the allele expression in primary fibroblasts.[18] We have verified by comparative DNA versus mRNA sequencing that, in primary myoblasts, the only expressed allele was that carrying the c.-32-13T > G mutation (Figure S8). Furthermore, after 3 days in differentiation culture conditions, these myoblasts could differentiate into multinucleated myotubes that accumulate glycogen in the lysosomal compartment. Under basal conditions myotubes from this patient retained about 20% of enzymatic activity when compared with WT cells (Figure S6B).

Following AMO addition, the splicing profile of the GAA mRNA of the patient-derived myotubes was first analyzed by endpoint PCR and compared to the profile obtained for myotubes derived from a healthy control (Figure 5A). Absolute percentage of inclusion of exon 2 compared to total GAA mRNA was also analyzed (Figure S7B). As shown in Figure 5A, the treatment of GSDII myotubes with AMOs

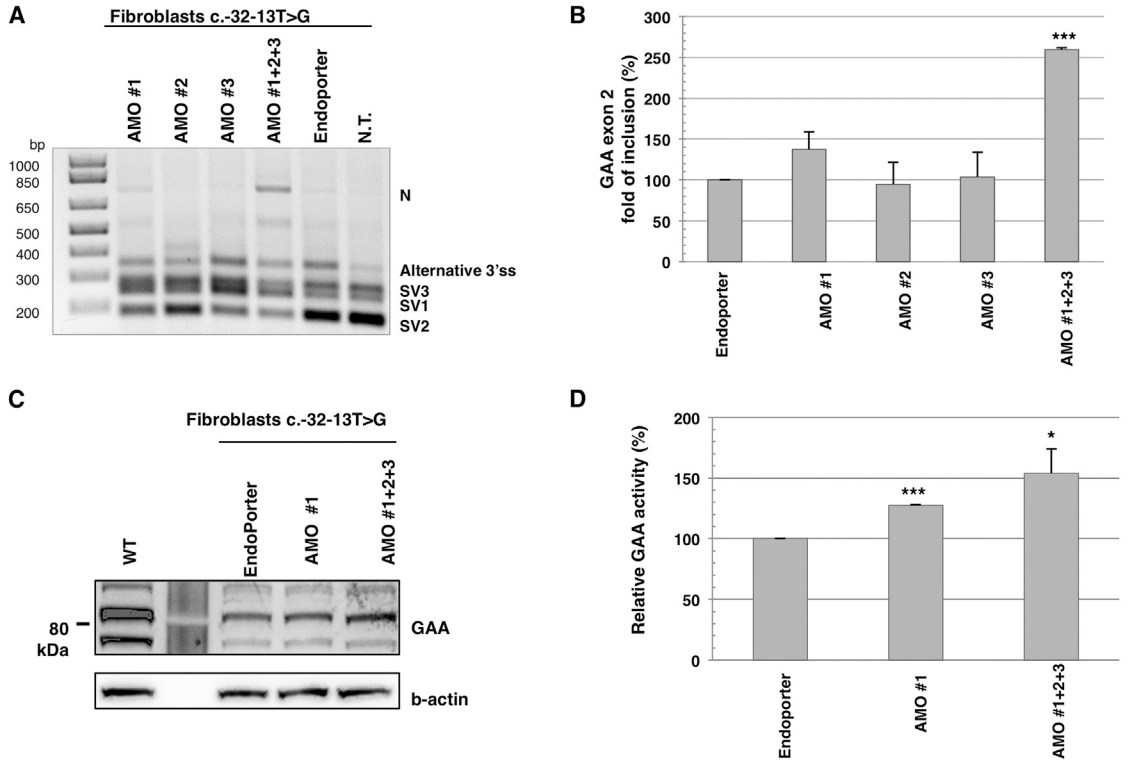

Figure 4. Effect of AMOs Targeting the 147–286 Region on Exon 2 Inclusion in Patient Fibroblasts

(A) RT-PCR analysis of patient fibroblasts carrying the c-32-13T > G transfected with AMOs 1, 2, and 3 delivered as single units or combined (1+2+3) to a final concentration of 15 μM. Cells transfected with Endo-Porter and not transfected (NT) were used as controls. The agarose gel picture shows a representative result of three independent experiments. (B) qRT-PCR analysis of *GAA* exon 2 inclusion (N) after AMO transfection in patient fibroblasts. The relative abundance of the N form is expressed as the fold of increase over fibroblasts treated with Endo-Porter reagent. qRT-PCR data are represented as mean ± SEM of three independent experiments (NS, not significant; ***$p < 0.001$). (C) Western blot analysis of endogenous mature GAA protein in patient fibroblasts after AMO treatment. Total protein extract was collected 72 hr after transfection with AMOs and analyzed with anti-GAA antibody. The western blot picture shows a representative result of three independent experiments. Beta actin protein was chosen as internal control. (D) GAA enzymatic activity in patient fibroblasts treated with AMOs was analyzed after 48 hr from transfection. Treatment with the Endo-Porter reagent was used as control. The GAA enzymatic activity data are represented as mean ± SEM of at least three independent experiments (*$p < 0.05$, ***$p < 0.001$).

1, 2, and 3 partially restored the correctly spliced variant of *GAA* mRNA. This qualitative observation was corroborated by real-time PCR that specifically demonstrated a 2-fold increase in the amount of the *GAA* exon 2 inclusion in AMO-treated myotubes compared to the mock-treated ones (Figure 5B). Again, as a consequence of this increase, in treated myotubes, 30% of total GAA mRNA was represented by the normal spliced GAA mRNA (Figure S7B). The increase of *GAA* at the mRNA level resulted in an approximately 40% increase in GAA enzymatic activity in AMO-treated GSDII myotubes over the mock-treated ones after 3 days of treatment (Figure 5C). These results indicated that the treatment with the combination of AMOs 1, 2, and 3 is also effective in patient-derived myotubes.

Finally, it was interesting to see whether a longer period of AMO treatment could have a functional effect on the reduction of aberrant glycogen storage in GSDII myotubes. Strikingly, after 1 week of treatment, the combination of AMOs 1, 2, and 3 resulted in a 70% increase of GAA activity and, most importantly, in a significant reduction of glycogen storage (Figures 5D and 5E).

DISCUSSION

The c.-32-13T > G mutation, within intron 1 of the GAA gene, is the most common mutation among patients affected by LO-GSDII, accounting for ~40%–70% of the alleles. Most LO patients carry this mutation in at least one allele.[6,18–22] We have previously shown that this single variant affects the binding of the U2AF65 splicing factor to the polypyrimidine tract of exon 2, leading to a complete or partial exclusion of this exon from the mature *GAA* mRNA.[26] However, patients carrying the c.-32-13T > G mutation also express variable levels of the normal spliced GAA transcript and protein. Thus, patients carrying this mutation retain some residual GAA activity that ranges from 1% to 30% of the activity present in healthy controls.[6,7,26]

The only approved treatment for GSDII is ERT with human recombinant GAA (hrGAA). Several studies support the efficacy of ERT in improving survival and stabilizing the disease course in patients affected by GSDII.[8,9] However, limitations of this approach in improving skeletal myopathy in patients affected by the LO

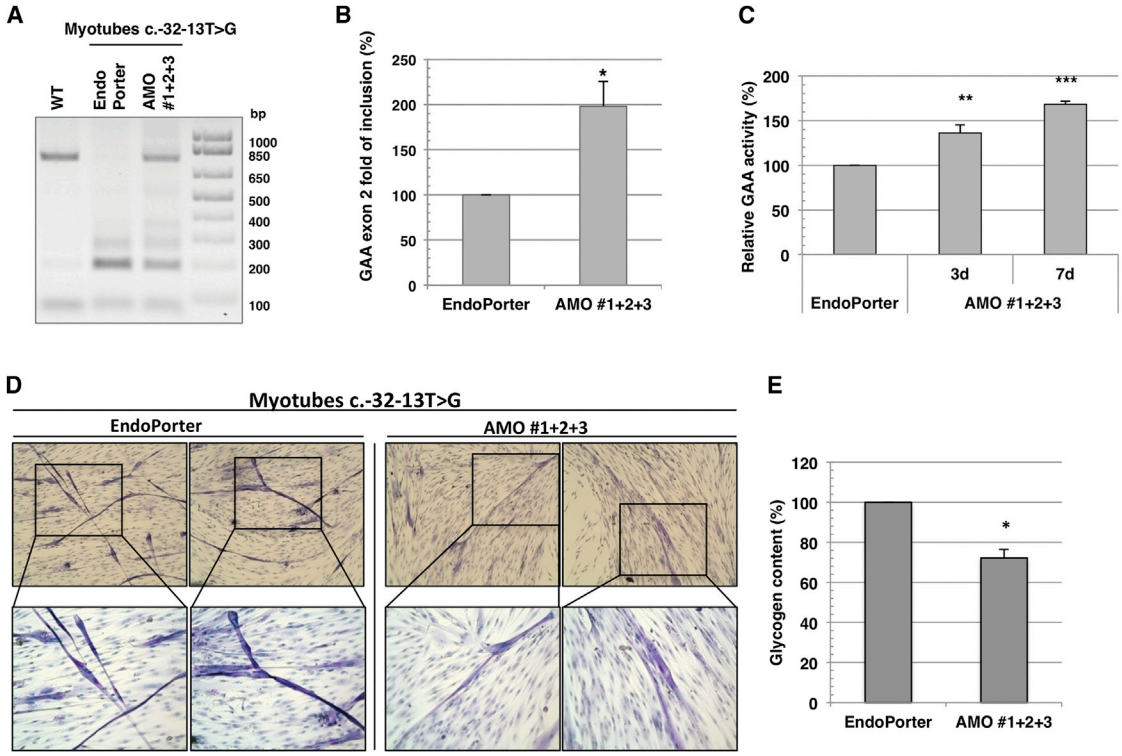

Figure 5. Reduction of Glycogen Accumulation in LO-GSDII Myotubes Carrying the c.-32-13T > G Mutation Treated with AMO 1+2+3

(A) *GAA* splicing profile assessed by RT-PCR in patient-derived myotubes treated with AMO 1+2+3 for 48 hr. WT myotubes were taken as positive control. The agarose picture is representative of two independent experiments. (B) qRT-PCR of the normal spliced (N) variant in LO-GSDII myotubes treated with AMO 1+2+3 for 48 hr. (C) GAA enzymatic activity in LO-GSDII myotubes treated with AMO 1+2+3 for 72 hr. (D) PAS staining of the LO-GSDII myotubes treated with AMO 1+2+3 for 7 days. The mock-treated LO-GSDII myotubes were taken as control. 10× magnification in the upper panels; 20× magnification in the lower panels. (D) Glycogen quantification in LO-GSDII myotubes treated with AMO 1+2+3 for 7 days using the fluorometric assay. The mock-treated LO-GSDII myotubes were taken as control. All data in (B), (C), and (E) are expressed as a percentage of the mock-treated LO-GSDII myotubes. In all experiments, the final combination AMO 1+2+3 was 15 μM. Data are represented in the graph as mean ± SEM of at least two independent experiments (*$p < 0.05$, **$p < 0.01$, ***$p < 0.001$).

phenotype are becoming evident.[10,11,33,34] At present, the only viable strategy that might be used, together with ERT, to improve its efficacy is the finding that overexpression of the TFEB transcription factor can lead to glycogen reduction in muscle cell cultures and mouse models of the disease.[35,36] Therefore, there is ample room for the search for additional effective therapies to be used as alternatives to or in combination with ERT.

Considering that the c.-32-13 T > G splicing mutation is extremely common among LO-GSDII patients, we decided to develop a personalized antisense oligonucleotide therapy to specifically correct the aberrant splicing of *GAA* exon 2 caused by this nucleotide variant. Antisense oligonucleotide technology has been shown to be a promising approach for splicing correction, and it has already entered clinical trial for several diseases, such as spinal muscular atrophy (SMA) and Duchenne muscular dystrophy (DMD).[28,29] Furthermore, with respect to *GAA*, antisense technology has been found to be effective in inhibiting the use of cryptic splice sites in various exons and introns of this gene that can become activated in the context of various pathogenic variants.[37]

In the specific case of the c.-32-13T > G mutation, this therapeutic strategy could be particularly effective, because only a partial rescue of the *GAA* exon 2 inclusion and enzymatic activity might be enough to achieve a beneficial clinical effect. It is widely accepted that levels above ~30% of the average GAA activity present in healthy controls would be sufficient to prevent the manifestation of the disease.[14,27]

In this work, we first used a minigene system (*GAA* exon 2 WT and MUT), bearing deletions of different regions of *GAA* exon 2, to identified potential silencer sequences within this exon. The deletion of 147–286 and 357–500 nt resulted in significant improvement of exon 2 inclusion in the minigene context, suggesting the presence of putative silencer elements within these regions (Figure 1). Both SpliceAid2 in silico analysis[30] and pull-down experiments confirmed the binding of negative splicing regulator factors belonging to the hnRNPs family to these regions. In particular, hnRNPA1/A2 and hnRNPH factors specifically bind regions 147–286 and 357–500, respectively (Figure 2). These data are in line with our previous findings showing that overexpression of hnRNPA1 and hnRNPH

produced a negative effect on exon 2 recognition, leading to an increase of exon 2 exclusion from the mature *GAA* transcript.[26]

Based on these results, we then designed a series of AMOs to specifically target both identified silencer sequences. An initial screening using a MUT minigene system led to the identification of a combination of 3 AMOs (1+2+3) directed toward the 147–286 exonic region as the best-performing strategy to rescue exon 2 inclusion. Treatment of minigene-expressing cells with this combination led to a 2.5-fold increase in the expression of the normal spliced *GAA* transcript (Figure 3). This result suggests the presence of a quite large inhibitory region within this sequence and/or the high binding affinity of hnRNP proteins.

A similar effect on exon 2 inclusion was observed in both fibroblasts (Figures 4A and 4B) and myotubes (Figures 5A and 5B) from patients carrying the c.-32-1T > G mutation (in compound heterozygosis with a null allele) after treatment with the combination of AMO 1+2+3. In these cells, the partial restoration of normal GAA splicing resulted in a significant increase of GAA enzymatic activity (Figures 4D and 5C).

Most importantly, in treated myotubes, a 70% increase of residual GAA activity was enough to partially correct the intracellular glycogen storage (Figures 5D and 5E). Under basal conditions, these myotubes retained quite high residual activity (about 25%) (Figure S6B). Therefore, in this case, a 70% increase of enzyme activity would be sufficient to exceed the threshold activity needed to partially clear out glycogen accumulation. These data suggest that in patients carrying the c.-32-13T > G mutation and retaining substantial residual GAA activity, this increase might be enough to achieve a beneficial effect in clinical settings.

Although these are encouraging results, further studies are needed to test the efficacy and the delivery of these AMOs to skeletal muscle in vivo. Several strategies aimed at improving antisense oligonucleotide delivery have been proposed,[38] including the use of a cell-penetrating peptide to target the skeletal muscle in a mouse model for GSDII.[39]

In conclusion, our results provide the first in vitro proof of principle for the use of AMOs to partially rescue normal splicing of c.-32-13T > G mutant alleles. Strikingly, AMO treatment was able to partially revert the pathologic phenotype in myotubes derived from a patient bearing the c.-32-13T > G mutation. To our knowledge, this is the first strategy that has achieved such a result, in addition to costly and rather ineffective (in adults) ERT. Therefore, these data suggest that the use of antisense oligonucleotide technology represents a promising strategy for the treatment of *GAA* patients carrying the common c.-32-13T > G mutation.

MATERIALS AND METHODS

Hybrid Minigene Constructs

The human WT GAA construct contains the exon 2 sequence and 50 nt of both flanking introns cloned inside the NdeI restriction site of the pTB hybrid minigene. The human MUT *GAA* construct was created from pTB *GAA* WT, using the hGAA-13Gs and hGAA-13Gas primers (Table S1) to introduce the single T-to-G substitution in position −13 of intron 1 by site-directed mutagenesis.[26] The constructs containing serial deletions (~140 nt) within exon 2 (GAA exon 2 deleted minigenes) were created by overlapping PCR mutagenesis with suitable primers (Table S1), using the pTB *GAA* WT minigene as a template. The constructs containing serial deletions within the pTB *GAA* MUT were obtained by introducing the single −13T/G substitution by site-directed mutagenesis, using pTB WT deleted minigenes as a template. The identity of each minigene was verified by sequence analysis.

Oligonucleotides

The sequence of all oligonucleotides (for mutagenesis, RT-PCR, qRT-PCR, pull-downs, and morpholino) is reported in Table S1.

Cell Culture and Transient Transfection

HeLa cells were grown in a complete medium made of high-glucose DMEM with GlutaMax I (Gibco) supplemented with 10% (v/v) fetal bovine serum (FBS) (Euroclone) and antibiotic antimycotic 1× solution (Sigma). For minigene transient transfection, 500 ng of each plasmid were transfected into 2.5×10^5 HeLa cells with Effectene reagent (QIAGEN).

Human primary fibroblasts were routinely cultured in high-glucose DMEM supplemented with 10% (v/v) FBS (Gibco), 2 mM glutamine (Euroclone), 100 U/mL penicillin G, and 100 μg/mL streptomycin (Euroclone). Cells were maintained at 37°C in a humidified atmosphere enriched with 5% (v/v) CO_2.

Skeletal Muscle Cell Differentiation

Primary myoblasts were routinely grown in Skeletal Muscle Cell Basal Medium (PromoCell) supplemented with 10% FBS (Gibco), 5% fetal calf serum (FCS), 50 μg/mL fetuin, 10 ng/mL epidermal growth factor (EGF), 1 ng/mL basic fibroblast growth factor (bFGF), 10 μg/mL insulin, 400 ng/mL dexamethasone, 2 mM glutamine, 100 U/mL penicillin G, and 100 μg/mL streptomycin and used up to the seventh passage. To induce skeletal muscle differentiation, primary myoblasts at 70% confluence were washed three times in PBS and shifted to freshly prepared DMEM 4.5 g/L glucose supplemented with 5% horse serum (Gibco), 10 μg/mL insulin, 100 U/mL penicillin G, and 100 μg/mL streptomycin. After 2 to 4 days in these culture conditions, the appearance of multinucleated myotubes was noted. Because these myotubes, unless innervated, were short lived in culture, the AMO treatment was begun simultaneously with the differentiation process.

RNA Extraction and Splicing Analysis

24 hr after transfection, total RNA was extracted from HeLa cells using EuroGold TriFast reagent (Euroclone), following the manufacturer's instructions. Then, 1 μg of total RNA was reverse transcribed using the specific primer Glo800 Rv, and the cDNA was amplified by PCR in a total volume of 50 μL using primers AlfaGlo2–3 Fw and Bra2 Rv (Table S1), specifically designed to amplify processed transcripts

derived from the minigene. The conditions used for the PCRs were 94°C for 3 min for the initial denaturation, 94°C for 45 s, 54°C for 45 s, 72°C for 1 min for 35 cycles, and 72°C for 10 min for the final extension. PCR products were resolved on 2% agarose gel and sequenced. Each transfection experiment was performed at least three times, and representative gels are shown in each case. Quantification of the intensity of the amplified products in agarose gels was done using ImageJ software. Total RNA from human primary fibroblasts or differentiated myotubes was extracted using TRIzol reagent (Ambion). For each sample, 1 μg of total RNA was retro-transcribed using the SuperScript III First-Strand Synthesis Kit (Invitrogen), following the manufacturer's instructions. To assess the splicing profile, cDNA was analyzed by endpoint PCR using the GoTaq DNA polymerase (Promega) and GAA Fw for and SKIP2 Rv primers (Table S1). The following conditions were used for amplification: 95°C for 3 min, 95°C for 30 s, 63°C for 30 s and 72°C for 48 s for 40 cycles, and 72°C for 7 min as final elongation. The PCR products were then resolved in a 1% agarose gel and visualized by trans-UV imaging.

AMO Transfection

AMOs were designed and ordered from Gene Tools (http://www.gene-tools.com). A standard fluoresceinated AMO (Gene Tools) was used as a control for testing both transfection specificity and delivery. Lyophilized oligonucleotides were resuspended in water to a final 1 mM concentration as a stock solution and stored at room temperature (RT). 6×10^4 HeLa cells were plated, 1 day before the transfection, in 12-well plates. AMO transfection was carried out with a final 15 μM concentration of oligonucleotide plus 6 μL of Endo-Porter reagent, according to the manufacturer's instructions. In the case of two or three oligonucleotides transfected together, the final concentration was always 15 μM. In the case of a fluoresceinated AMO, the final concentration was 10 μM. Cells were co-transfected with pTB GAA WT and MUT minigenes (250 ng) using Effectene reagent (QIAGEN). After 48 hr, total RNA was extracted using EuroGold TriFastreagent (Euroclone); 1 μg of total RNA was reverse transcribed and amplified by PCR, as described earlier. $3 \times 10^4/cm^2$ human primary fibroblasts were seeded in 6-well plates (for the analysis of mRNA expression) or in 60 mm Petri dishes (for western blot analysis and enzymatic activity measurement). AMO transfection was performed as outlined earlier. The treatments were stopped at 48 hr for the analysis of mRNA expression or at 72 hr for western blot analysis and enzyme activity measurement.

Real-Time PCR

The abundance of GAA exon 2 inclusion of transfected pTB GAA WT and MUT minigenes, with and without AMO treatment, were analyzed by real-time qPCR using the primers F3 Fw and R3 Rv specific for fibronectin exon EDA −1 and GAA exon 2 of the pTB minigenes. Amplification of AlfaGlo2–3, deriving from the same mRNA and produced by the pTB hybrid minigene, was used as an internal reference gene using the following oligonucleotides: AlfaGlo2 142 Fw and AlfaGlo2–3 294 Rv. The amount of normal spliced mRNA of pTB MUT GAA exon 2 was taken as a reference sample and considered to be 1. At least three independent determinations for each condition were performed. Real-time PCR was performed using the CFX96 thermal cycler and the IQ SYBR Green Supermix (Bio-Rad), following the manufacturer's instructions. Standard curves were prepared for the target and internal reference gene to obtain the efficiency of the primers. To verify the specificity of the amplification, a melt-curve analysis was performed; no specific PCR products were present. The quantification was made using the Pfaffl ΔΔCt equation. The abundance of endogenous GAA exon 2 inclusion (N) in human primary fibroblasts and myoblasts was determined by real-time PCR using Sso Advance Universal SYBR Green Supermix (Bio-Rad) and the specific primers GAA ex1–2 Fw and Rv. The relative GAA exon 2 inclusion was obtained by normalizing on housekeeping gene HPRT and the HPRT Fw and HPRT Rv primers, using the Pfaffl ΔΔCt equation. The amount of normal spliced (N) mRNA of human primary fibroblasts and myoblasts, carrying the c.-32-13T > G mutation, was taken as the reference sample and considered to be 1. The absolute GAA exon 2 inclusion was obtained by normalizing on GAA exon 18–19 mRNA using primers GAA ex18–19 Fw and Rv. Real-time PCR was performed on a LightCycler 480 Real-Time PCR system (Roche).

Pull-Down Assay

The DNA template, used for RNA in vitro transcription, was obtained by PCR on the pTB WT minigene with the following primer couples: T7 147–286 Fw and 147–286 Rv, T7 357–500 Fw and 357–500 Rv, and T7 and 427–571 Fw and 427–571 Rv. The T7 RNA polymerase promoter sequence was added to all forward primers. The PCR products were then used for generating the pull-down target RNAs by T7 RNA polymerase (Agilent) transcription in vitro, according to the manufacturer's instructions. Then, the pull-down protocol was performed as previously reported.[40] Briefly, 2 μg of target RNA were placed in 400 μL of a reaction mixture containing 100 mM NaOAC (pH 5.0) and 5 mM sodium m-periodate (Sigma), incubated for 1 hr in the dark at RT, ethanol precipitated, and finally resuspended in 100 μL of 100 mM NaOAC (pH 5.0). Approximately 100 μL of adipic acid dehydrazide agarose beads in a 50% slurry (Sigma) previously equilibrated with 100 mM NaOAC (pH 5.2) were added to each periodate-treated RNA, and the mix was incubated for 12 hr at 4°C on a rotator in the dark. The beads with the bound RNA were then washed with 2 M NaCl and equilibrated in 1× washing buffer (20 mM HEPES [pH 7.5], 100 mM KCl, 0.2 mM EDTA, 0.5 mM DTT, 6% glycerol). Then, the beads were incubated, in a final volume of 500 μL, with 1 mg of HeLa cell nuclear extract (4C Biotech), 1× washing buffer, and heparin (final concentration of 1 μg/μL) for 30 min on a rotator at RT. The beads were then washed with 1× washing buffer before addition of SDS sample buffer and loading on SDS-10% polyacrylamide gels. Proteins were visualized by colloidal Coomassie G-250 (Sigma) staining. Proteins of interest were excised from the gel and analyzed by mass spectrometry by Alta Bioscience (https://altabioscience.com/).

Western Blot Analysis

Total protein extracts were dissolved in standard 4× SDS loading buffer and were heated for 5 min at 94°C before loading on a 10%

SDS-polyacrylamide denaturing gel. The gel was then electroblotted onto a Hybond-C Extra membrane (Amersham) according to standard protocols (Amersham). For pull-down samples, membranes were stained with Ponceau (Sigma) before blocking with 5% skim milk (non-fat dry milk in 1× PBS, 0.1% Tween 20). In the special case of SRSF recognition, membranes were incubated using western blocking reagent 1× solution (Roche), according to the manufacturer's instructions. Anti-SRSF antibody (1H4) was purchased from Invitrogen and diluted 1:1,000 in western blocking reagent 0.5× solution. The antibodies Anti-Syncript/hnRNPQ (Sigma) and hnRNPR (Abcam) were used at a final dilution of 1:500. Polyclonal rabbit antibodies against hnRNPA1/A2 (1:1000) and hnRNPH (1:500) were homemade in the International Centre for Genetic Engineering and Biotechnology (ICGEB) using standard immunization protocols. Membranes targeted for endogenous GAA protein were probed with an antiserum against GAA, as described elsewhere,[41] and the signals were normalized to those obtained with anti-actin primary antibody (Sigma) used at a 1:1,000 dilution. Proteins probed with different primary antibodies were then incubated with anti-rabbit or anti-mouse horseradish peroxidase (HPR)-conjugated antibodies (Dako) to a final 1:2,000 dilution and detected with a chemiluminescence kit, ECL STAR (Pierce Biotechnology), according to the manufacturer's instructions. In the particular case of SRSF detection, the Super Signal West Femto kit was used (Thermo Scientific). FireReader v.4 (Uvitec) was used as the gel documentation system.

Enzymatic Activity

GAA enzymatic activity was measured as previously reported,[42] using 4-methylumbelliferyl-α-D-glucopiranoside (Glycosinth) as a substrate. Briefly, 72 hr from AMO treatment, primary fibroblasts were harvested, washed once in PBS, resuspended in 80 μL of water, and sonicated twice at an ice-cold temperature. Total protein concentration in cell lysates was measured by the Lowry method. 30 μg of total protein were mixed with 10 μL of 2 mM 4-methylumbelliferyl-α-D-glucopiranoside in acetate buffer in a final volume of 20 μL and incubated at 37°C for 1 hr. The reaction was stopped by the addition of 1,980 μL of 0.5 M carbonate buffer (pH 10.7). The resulting fluorescence was measured at 355 and 460 nm excitation (Ex) and emission (Em) using a Gemini microplate reader (Molecular Devices). All assays were done in triplicate.

Periodic Acid-Schiff Staining

Periodic acid-Schiff (PAS) staining was employed to detect glycogen accumulation. After 7 days of treatment with AMOs 1, 2, and 3, primary myotubes were fixed in 4% paraformaldehyde (PFA) for 20 min, extensively washed, and mounted face up on a coverslip. Samples were oxidized in 1% periodic acid for 5 min, rinsed three times in distilled water, and treated with Schiff's reagent for 25 min. After extensive washing, slides were stained with Mayer's hematoxylin for 10 min.

Glycogen Fluorometric Assay

Glycogen quantification in patient myotubes was performed using the glycogen colorimetric or fluorometric assay kit (BioVision), following the manufacturer's instructions. Briefly, after 7 days of treatment with AMOs 1, 2, and 3, primary myotubes were harvested, washed once in PBS, resuspended in 60 μL of water, and sonicated twice at an ice-cold temperature. The total lysate was boiled for 10 min to inactivate the glycogen-degrading enzymes and centrifuged at 18,000 × *g* for 10 min at 4°C. 2 μL of the supernatant were mixed with 1 μL of hydrolysis enzyme mix in a total volume of 50 μL of hydrolysis buffer and incubated for 30 min at RT. 50 μL of the reaction enzyme mix were then added, and the reaction was incubated for another 30 min in the dark. The resulting fluorescence (Ex/Em = 535/587 nm) was recorded using a Gemini microplate reader (Molecular Devices).

Bioinformatic Analysis

SpliceAid2 was used as the bioinformatic tool for splicing factor binding prediction (http://www.introni.it/spliceaid.html).[30] HSF3 (http://www.umd.be/HSF3/)[31] was also used in the analysis; it includes several algorithms for predicting enhancer and silencer elements.

Statistics

Statistical analyses were performed with Microsoft Excel for PC 2013. Significant differences in expression levels of GAA exon 2 (N), GAA protein, GAA enzymatic activity, and glycogen quantification were analyzed by Student's unpaired t test.

Normal distribution of data (Table S2) was assessed using the Shapiro-Wilk test web version (http://scistatcalc.blogspot.it/2013/10/shapiro-wilk-test-calculator.html).

SUPPLEMENTAL INFORMATION

Supplemental Information includes eight figures and two tables and can be found with this article online at http://dx.doi.org/10.1016/j.ymthe.2017.05.019.

AUTHOR CONTRIBUTIONS

E.G. and P.P. conducted the experiments and analyzed the data. E.B. and A.D. designed the experiments and supervised the project. All authors participated in writing the manuscript.

CONFLICTS OF INTEREST

The authors declare no conflict of interest.

ACKNOWLEDGMENTS

This work was supported by Telethon grant GGP14192 for identification of new therapeutic agents for the treatment of glycogenosis type 2 due to the common splicing mutation c.-32-13T > G. The EuroBioBank and Telethon Network Genetic Biobanks (GTB12001F) are acknowledged for providing biological samples.

REFERENCES

1. Hirschhorn, R., and Reuser, A.J. (2001). Glycogen storage disease type II: acid a-glucosidase (acid maltase) deficiency. In The Metabolic and Molecular Basis of

Inherited Disease, Vol. III, C.R. Scriver, A.L. Beaudet, W.S. Sly, and D. Valle, eds. (McGraw-Hill), pp. 3389–3420.

2. Güngör, D., and Reuser, A.J. (2013). How to describe the clinical spectrum in Pompe disease? Am. J. Med. Genet. A. *161A*, 399–400.
3. Kishnani, P.S., Hwu, W.L., Mandel, H., Nicolino, M., Yong, F., and Corzo, D.; Infantile-Onset Pompe Disease Natural History Study Group (2006). A retrospective, multinational, multicenter study on the natural history of infantile-onset Pompe disease. J. Pediatr. *148*, 671–676.
4. van den Hout, H.M., Hop, W., van Diggelen, O.P., Smeitink, J.A., Smit, G.P., Poll-The, B.T., Bakker, H.D., Loonen, M.C., de Klerk, J.B., Reuser, A.J., and van der Ploeg, A.T. (2003). The natural course of infantile Pompe's disease: 20 original cases compared with 133 cases from the literature. Pediatrics *112*, 332–340.
5. Hagemans, M.L., Winkel, L.P., Van Doorn, P.A., Hop, W.J., Loonen, M.C., Reuser, A.J., and Van der Ploeg, A.T. (2005). Clinical manifestation and natural course of late-onset Pompe's disease in 54 Dutch patients. Brain *128*, 671–677.
6. Herzog, A., Hartung, R., Reuser, A.J., Hermanns, P., Runz, H., Karabul, N., Gökce, S., Pohlenz, J., Kampmann, C., Lampe, C., et al. (2012). A cross-sectional single-centre study on the spectrum of Pompe disease, German patients: molecular analysis of the GAA gene, manifestation and genotype-phenotype correlations. Orphanet J. Rare Dis. *7*, 35.
7. Schüller, A., Wenninger, S., Strigl-Pill, N., and Schoser, B. (2012). Toward deconstructing the phenotype of late-onset Pompe disease. Am. J. Med. Genet. C. Semin. Med. Genet. *160C*, 80–88.
8. Nicolino, M., Byrne, B., Wraith, J.E., Leslie, N., Mandel, H., Freyer, D.R., Arnold, G.L., Pivnick, E.K., Ottinger, C.J., Robinson, P.H., et al. (2009). Clinical outcomes after long-term treatment with alglucosidase alfa in infants and children with advanced Pompe disease. Genet. Med. *11*, 210–219.
9. Chen, L.R., Chen, C.A., Chiu, S.N., Chien, Y.H., Lee, N.C., Lin, M.T., Hwu, W.L., Wang, J.K., and Wu, M.H. (2009). Reversal of cardiac dysfunction after enzyme replacement in patients with infantile-onset Pompe disease. J. Pediatr. *155*, 271–275.
10. van der Ploeg, A.T., Clemens, P.R., Corzo, D., Escolar, D.M., Florence, J., Groeneveld, G.J., Herson, S., Kishnani, P.S., Laforet, P., Lake, S.L., et al. (2010). A randomized study of alglucosidase alfa in late-onset Pompe's disease. N. Engl. J. Med. *362*, 1396–1406.
11. Strothotte, S., Strigl-Pill, N., Grunert, B., Kornblum, C., Eger, K., Wessig, C., Deschauer, M., Breunig, F., Glocker, F.X., Vielhaber, S., et al. (2010). Enzyme replacement therapy with alglucosidase alfa in 44 patients with late-onset glycogen storage disease type 2: 12-month results of an observational clinical trial. J. Neurol. *257*, 91–97.
12. Wisselaar, H.A., Kroos, M.A., Hermans, M.M., van Beeumen, J., and Reuser, A.J. (1993). Structural and functional changes of lysosomal acid alpha-glucosidase during intracellular transport and maturation. J. Biol. Chem. *268*, 2223–2231.
13. Byrne, B.J., Kishnani, P.S., Case, L.E., Merlini, L., Müller-Felber, W., Prasad, S., and van der Ploeg, A. (2011). Pompe disease: design, methodology, and early findings from the Pompe Registry. Mol. Genet. Metab. *103*, 1–11.
14. Kroos, M., Hoogeveen-Westerveld, M., Michelakakis, H., Pomponio, R., Van der Ploeg, A., Halley, D., and Reuser, A.; GAA Database Consortium (2012). Update of the Pompe disease mutation database with 60 novel GAA sequence variants and additional studies on the functional effect of 34 previously reported variants. Hum. Mutat. *33*, 1161–1165.
15. Becker, J.A., Vlach, J., Raben, N., Nagaraju, K., Adams, E.M., Hermans, M.M., Reuser, A.J., Brooks, S.S., Tifft, C.J., Hirschhorn, R., et al. (1998). The African origin of the common mutation in African American patients with glycogen-storage disease type II. Am. J. Hum. Genet. *62*, 991–994.
16. Lin, C.Y., and Shieh, J.J. (1996). Molecular study on the infantile form of Pompe disease in Chinese in Taiwan. Zhonghua Min Guo Xiao Er Ke Yi Xue Hui Za Zhi *37*, 115–121.
17. Ausems, M.G., Verbiest, J., Hermans, M.P., Kroos, M.A., Beemer, F.A., Wokke, J.H., Sandkuijl, L.A., Reuser, A.J., and van der Ploeg, A.T. (1999). Frequency of glycogen storage disease type II in the Netherlands: implications for diagnosis and genetic counselling. Eur. J. Hum. Genet. *7*, 713–716.
18. Montalvo, A.L., Bembi, B., Donnarumma, M., Filocamo, M., Parenti, G., Rossi, M., Merlini, L., Buratti, E., De Filippi, P., Dardis, A., et al. (2006). Mutation profile of the GAA gene in 40 Italian patients with late onset glycogen storage disease type II. Hum. Mutat. *27*, 999–1006.
19. Nascimbeni, A.C., Fanin, M., Tasca, E., and Angelini, C. (2008). Molecular pathology and enzyme processing in various phenotypes of acid maltase deficiency. Neurology *70*, 617–626.
20. Gort, L., Coll, M.J., and Chabás, A. (2007). Glycogen storage disease type II in Spanish patients: high frequency of c.1076-1G>C mutation. Mol. Genet. Metab. *92*, 183–187.
21. Wan, L., Lee, C.C., Hsu, C.M., Hwu, W.L., Yang, C.C., Tsai, C.H., and Tsai, F.J. (2008). Identification of eight novel mutations of the acid alpha-glucosidase gene causing the infantile or juvenile form of glycogen storage disease type II. J. Neurol. *255*, 831–838.
22. Joshi, P.R., Gläser, D., Schmidt, S., Vorgerd, M., Winterholler, M., Eger, K., Zierz, S., and Deschauer, M. (2008). Molecular diagnosis of German patients with late-onset glycogen storage disease type II. J. Inherit. Metab. Dis. *31* (*Suppl 2*), S261–S265.
23. Huie, M.L., Chen, A.S., Tsujino, S., Shanske, S., DiMauro, S., Engel, A.G., and Hirschhorn, R. (1994). Aberrant splicing in adult onset glycogen storage disease type II (GSDII): molecular identification of an IVS1 (-13T–>G) mutation in a majority of patients and a novel IVS10 (+1GT–>CT) mutation. Hum. Mol. Genet. *3*, 2231–2236.
24. Boerkoel, C.F., Exelbert, R., Nicastri, C., Nichols, R.C., Miller, F.W., Plotz, P.H., and Raben, N. (1995). Leaky splicing mutation in the acid maltase gene is associated with delayed onset of glycogenosis type II. Am. J. Hum. Genet. *56*, 887–897.
25. Raben, N., Nichols, R.C., Martiniuk, F., and Plotz, P.H. (1996). A model of mRNA splicing in adult lysosomal storage disease (glycogenosis type II). Hum. Mol. Genet. *5*, 995–1000.
26. Dardis, A., Zanin, I., Zampieri, S., Stuani, C., Pianta, A., Romanello, M., Baralle, F.E., Bembi, B., and Buratti, E. (2014). Functional characterization of the common c.-32-13T>G mutation of GAA gene: identification of potential therapeutic agents. Nucleic Acids Res. *42*, 1291–1302.
27. Kroos, M.A., Pomponio, R.J., Hagemans, M.L., Keulemans, J.L., Phipps, M., DeRiso, M., Palmer, R.E., Ausems, M.G., Van der Beek, N.A., Van Diggelen, O.P., et al. (2007). Broad spectrum of Pompe disease in patients with the same c.-32-13T->G haplotype. Neurology *68*, 110–115.
28. Singh, N.N., Lee, B.M., DiDonato, C.J., and Singh, R.N. (2015). Mechanistic principles of antisense targets for the treatment of spinal muscular atrophy. Future Med. Chem. *7*, 1793–1808.
29. Koo, T., and Wood, M.J. (2013). Clinical trials using antisense oligonucleotides in Duchenne muscular dystrophy. Hum. Gene Ther. *24*, 479–488.
30. Piva, F., Giulietti, M., Burini, A.B., and Principato, G. (2012). SpliceAid 2: a database of human splicing factors expression data and RNA target motifs. Hum. Mutat. *33*, 81–85.
31. Desmet, F.O., Hamroun, D., Lalande, M., Collod-Béroud, G., Claustres, M., and Béroud, C. (2009). Human Splicing Finder: an online bioinformatics tool to predict splicing signals. Nucleic Acids Res. *37*, e67.
32. Havens, M.A., and Hastings, M.L. (2016). Splice-switching antisense oligonucleotides as therapeutic drugs. Nucleic Acids Res. *44*, 6549–6563.
33. Kishnani, P.S., and Beckemeyer, A.A. (2014). New therapeutic approaches for Pompe disease: enzyme replacement therapy and beyond. Pediatr. Endocrinol. Rev. *12* (*Suppl 1*), 114–124.
34. Toscano, A., and Schoser, B. (2013). Enzyme replacement therapy in late-onset Pompe disease: a systematic literature review. J. Neurol. *260*, 951–959.
35. Sato, Y., Kobayashi, H., Higuchi, T., Shimada, Y., Ida, H., and Ohashi, T. (2016). TFEB overexpression promotes glycogen clearance of Pompe disease iPSC-derived skeletal muscle. Mol. Ther. Methods Clin. Dev. *3*, 16054.
36. Spampanato, C., Feeney, E., Li, L., Cardone, M., Lim, J.A., Annunziata, F., Zare, H., Polishchuk, R., Puertollano, R., Parenti, G., et al. (2013). Transcription factor EB (TFEB) is a new therapeutic target for Pompe disease. EMBO Mol. Med. *5*, 691–706.
37. Bergsma, A.J., In 't Groen, S.L., Verheijen, F.W., van der Ploeg, A.T., and Pijnappel, W.P. (2016). From cryptic toward canonical pre-mRNA splicing in Pompe disease: a pipeline for the development of antisense oligonucleotides. Mol. Ther. Nucleic Acids *5*, e361.

38. Juliano, R.L. (2016). The delivery of therapeutic oligonucleotides. Nucleic Acids Res. *44*, 6518–6548.

39. Clayton, N.P., Nelson, C.A., Weeden, T., Taylor, K.M., Moreland, R.J., Scheule, R.K., Phillips, L., Leger, A.J., Cheng, S.H., and Wentworth, B.M. (2014). Antisense oligonucleotide-mediated suppression of muscle glycogen synthase 1 synthesis as an approach for substrate reduction therapy of Pompe disease. Mol. Ther. Nucleic Acids *3*, e206.

40. Prudencio, M., Jansen-West, K.R., Lee, W.C., Gendron, T.F., Zhang, Y.J., Xu, Y.F., Gass, J., Stuani, C., Stetler, C., Rademakers, R., et al. (2012). Misregulation of human sortilin splicing leads to the generation of a nonfunctional progranulin receptor. Proc. Natl. Acad. Sci. USA *109*, 21510–21515.

41. Montalvo, A.L., Cariati, R., Deganuto, M., Guerci, V., Garcia, R., Ciana, G., Bembi, B., and Pittis, M.G. (2004). Glycogenosis type II: identification and expression of three novel mutations in the acid alpha-glucosidase gene causing the infantile form of the disease. Mol. Genet. Metab. *81*, 203–208.

42. Hermans, M.M., Kroos, M.A., van Beeumen, J., Oostra, B.A., and Reuser, A.J. (1991). Human lysosomal alpha-glucosidase. Characterization of the catalytic site. J. Biol. Chem. *266*, 13507–13512.

YMTHE, Volume *25*

Supplemental Information

Glycogen Reduction in Myotubes of Late-Onset Pompe Disease Patients Using Antisense Technology

Elisa Goina, Paolo Peruzzo, Bruno Bembi, Andrea Dardis, and Emanuele Buratti

Figure S1.

a

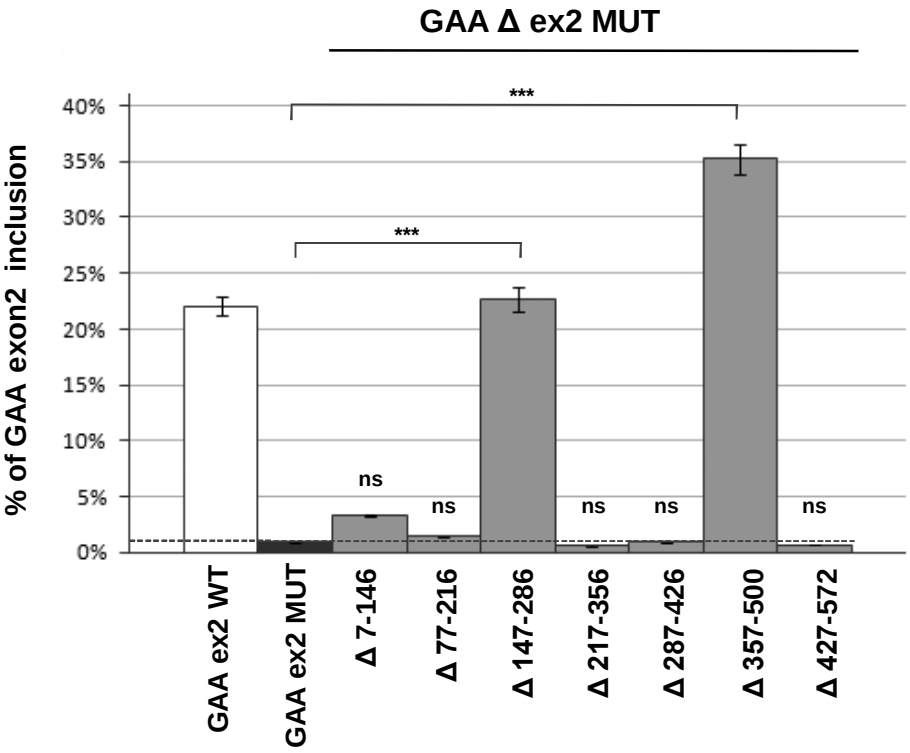

b

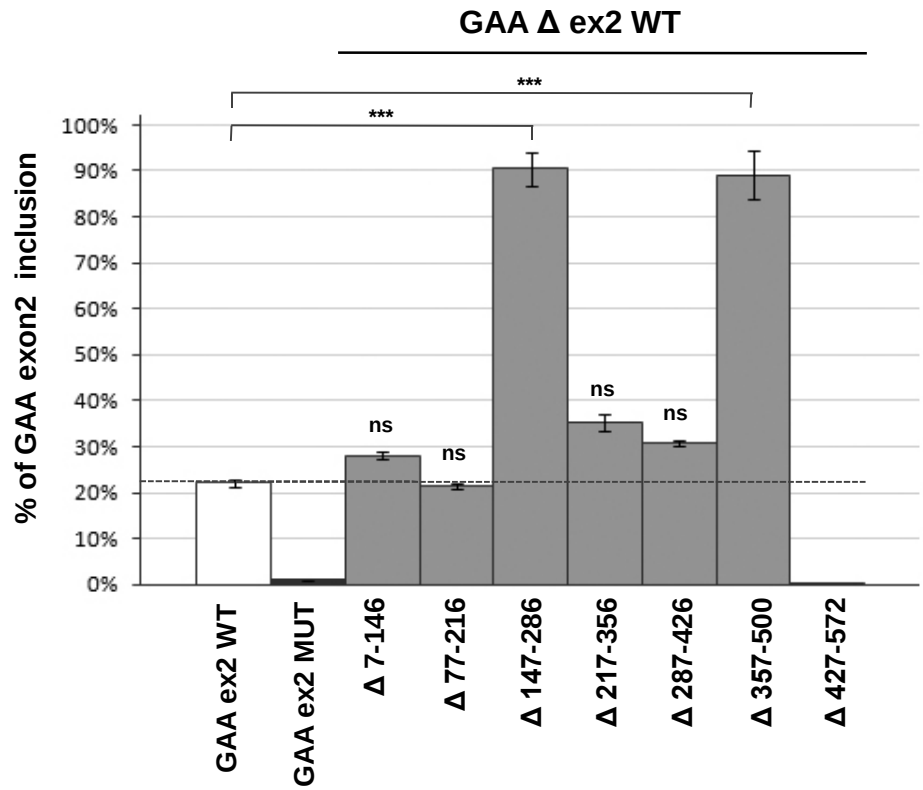

c

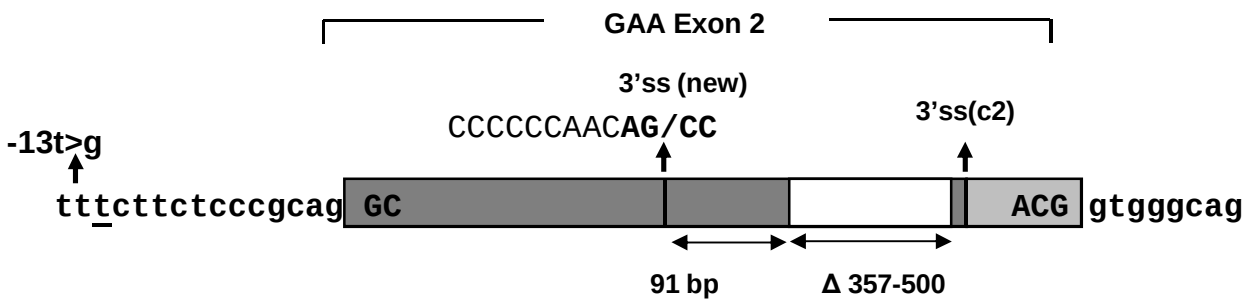

Figure S2.

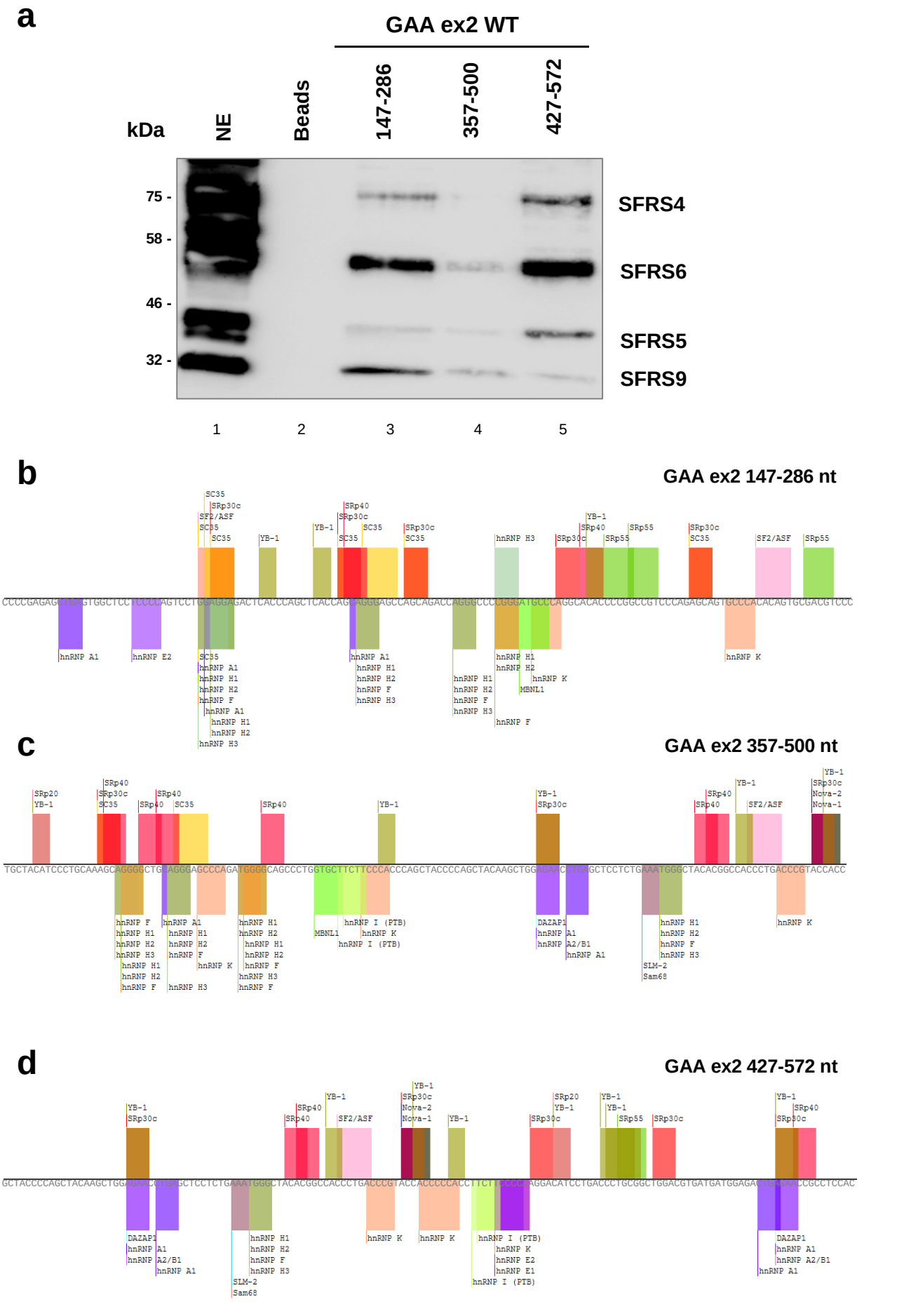
a
GAA ex2 WT
kDa
NE
Beads
147-286
357-500
427-572
75 -
58 -
46 -
32 -
SFRS4
SFRS6
SFRS5
SFRS9
1
2
3
4
5
b
GAA ex2 147-286 nt
c
GAA ex2 357-500 nt
d
GAA ex2 427-572 nt

Figure S3.

a

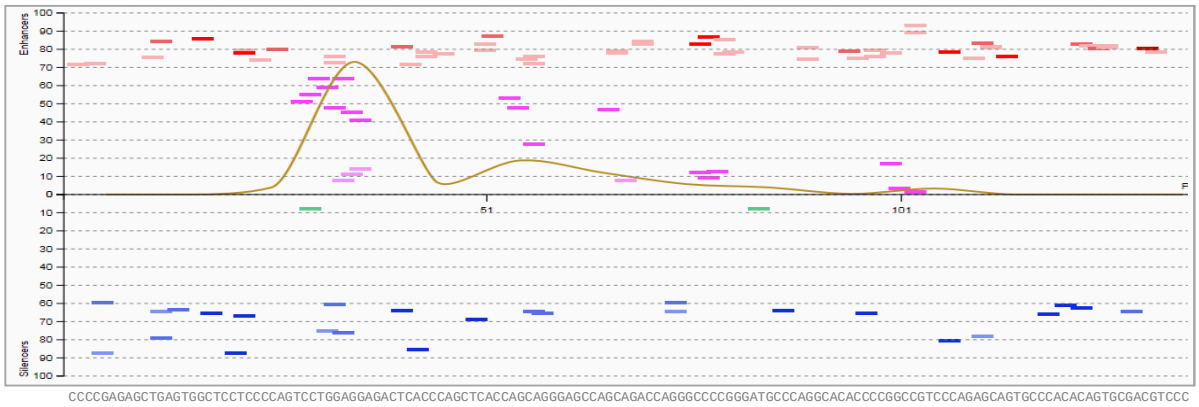

b

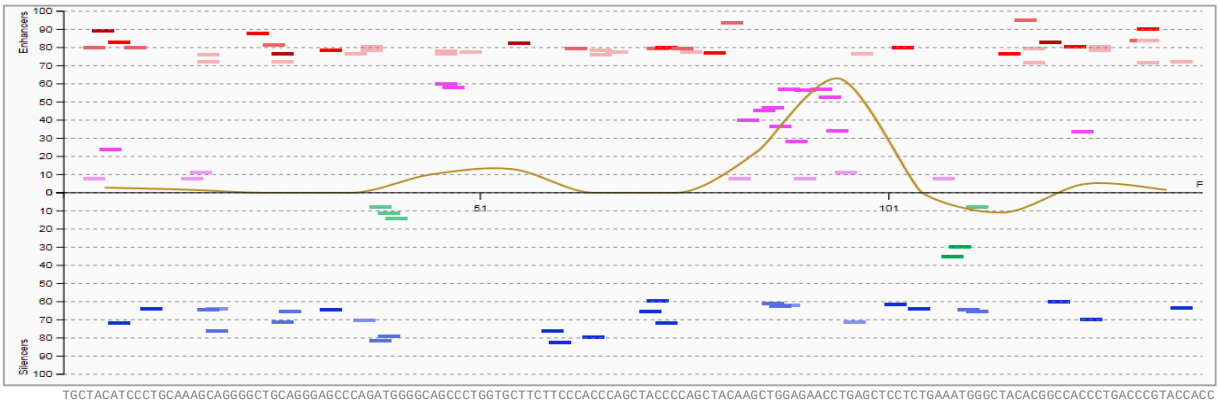

c

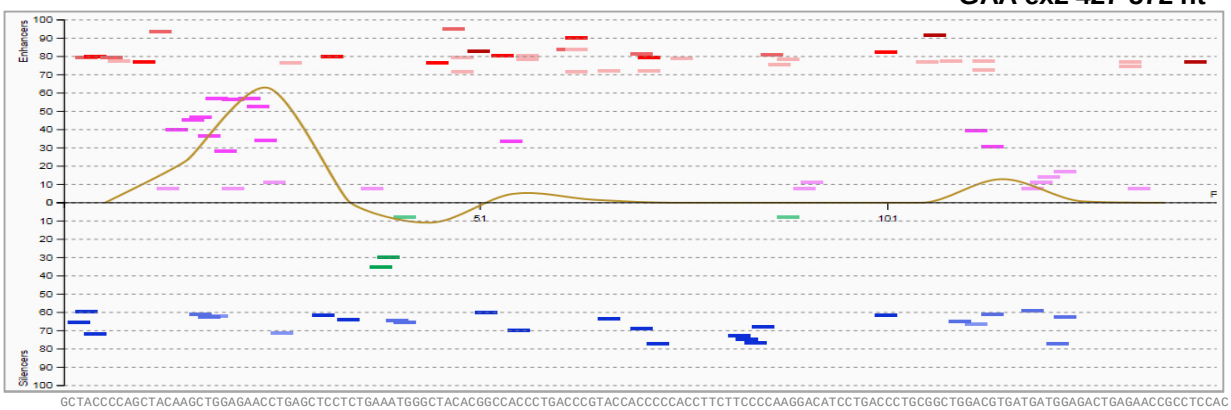

d

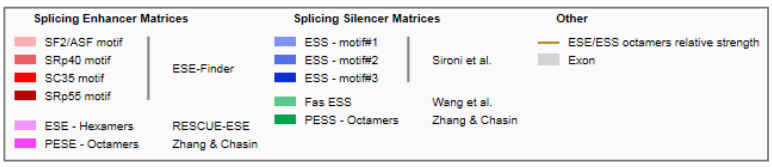

Figure S4.

a

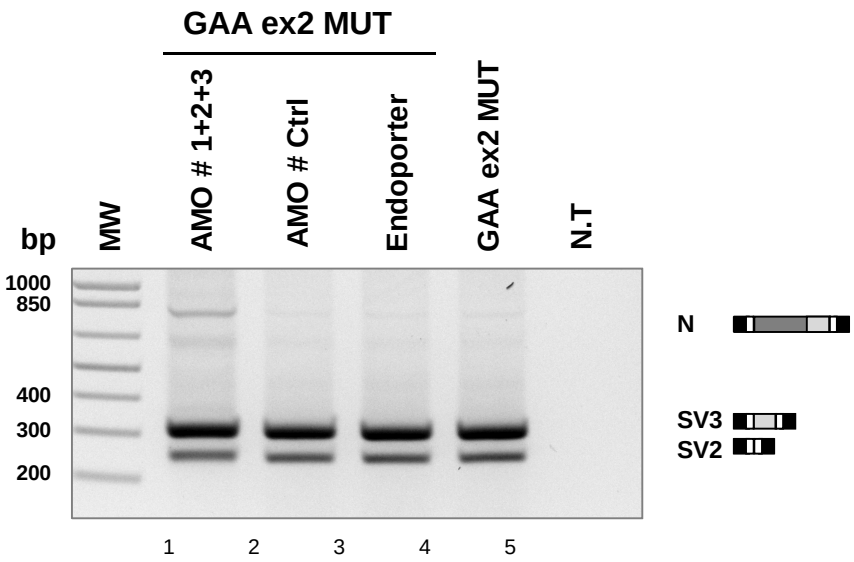
GAA ex2 MUT
bp
MW
AMO # 1+2+3
AMO # Ctrl
Endoporter
GAA ex2 MUT
N.T
1000
850
400
300
200
N
SV3
SV2
1
2
3
4
5

b

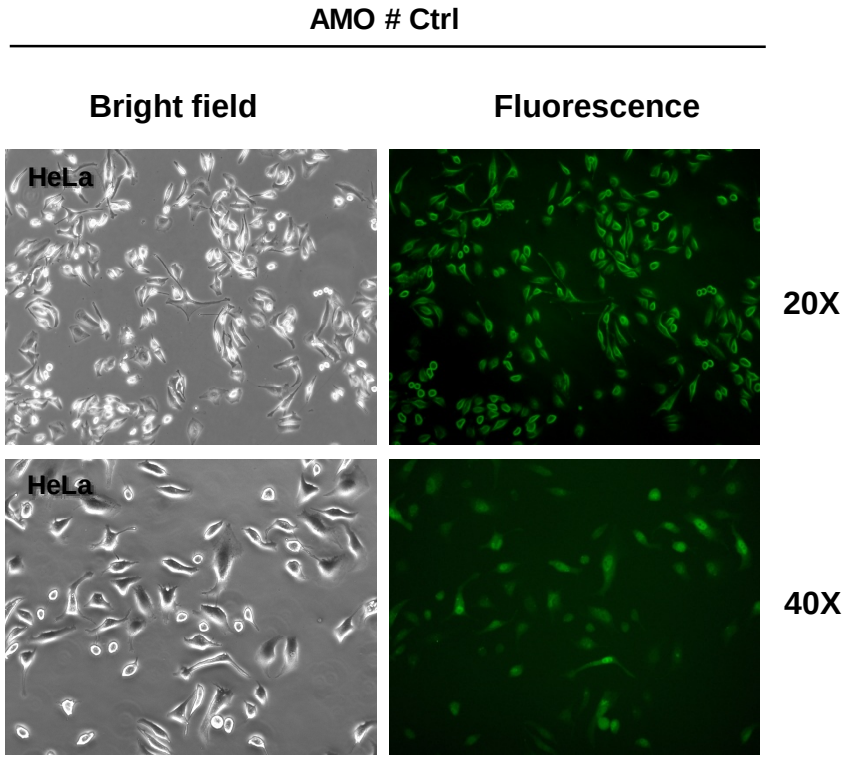
AMO # Ctrl
Bright field
Fluorescence
HeLa
HeLa
20X
40X

Figure S5.

a

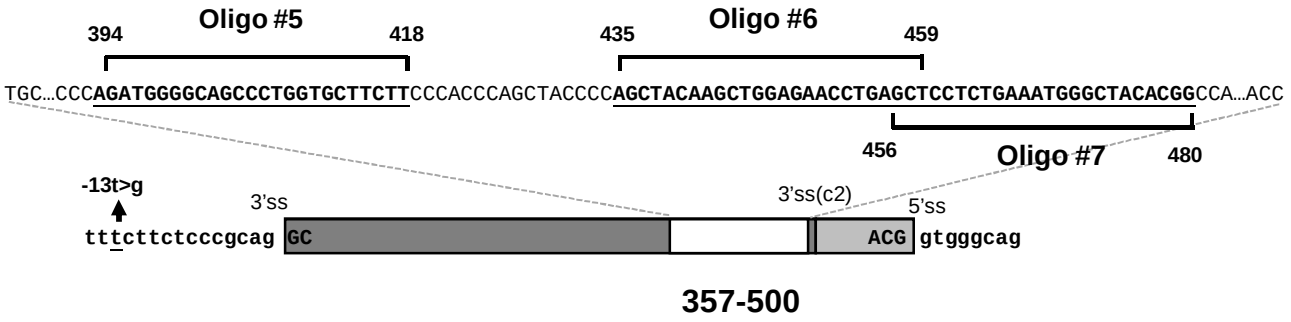

b

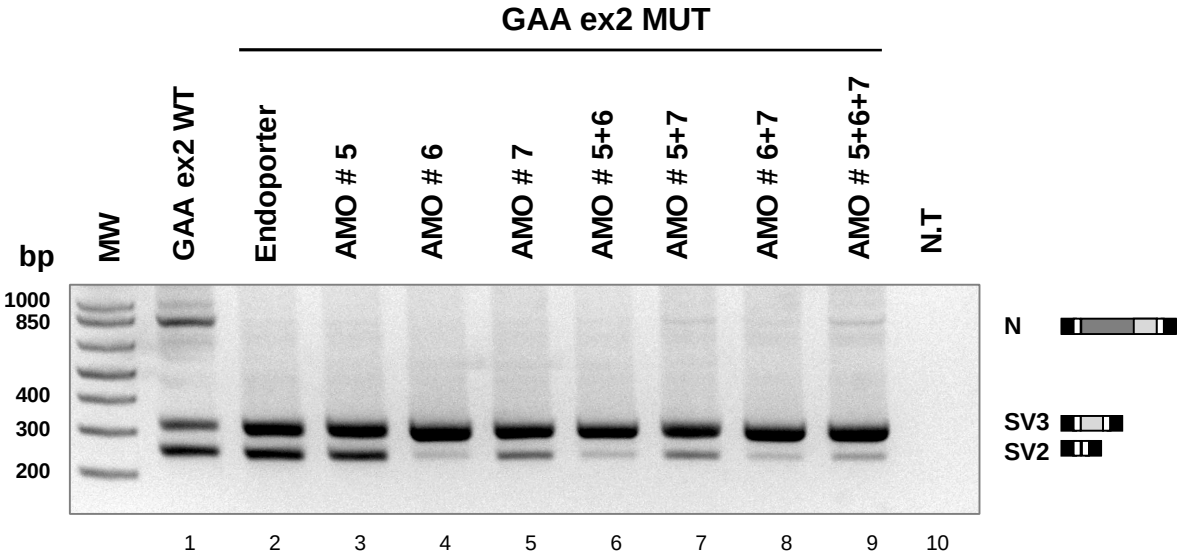

c

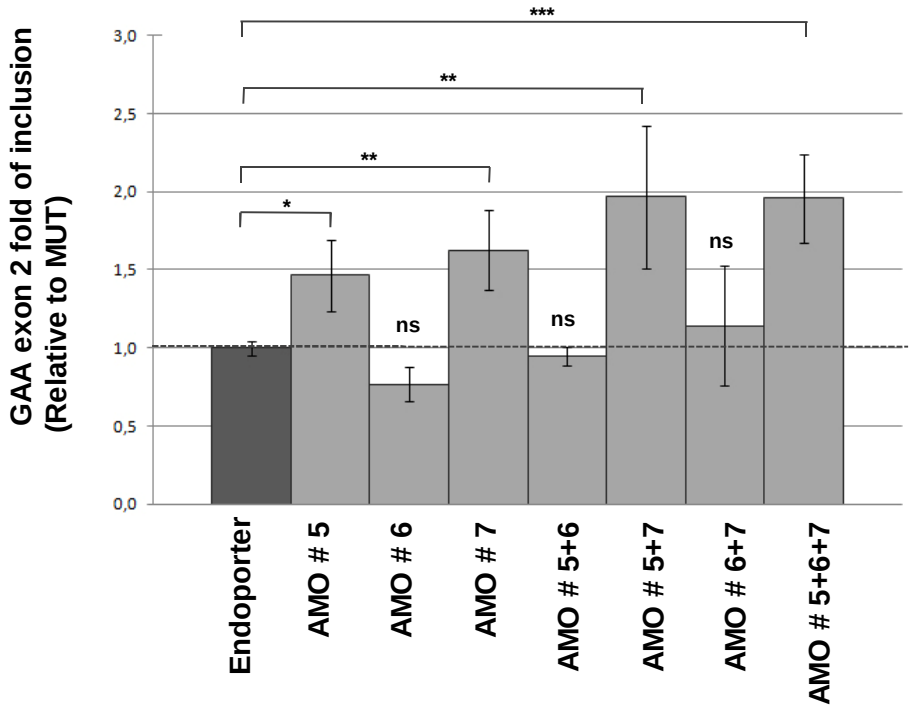

Figure S6.

a

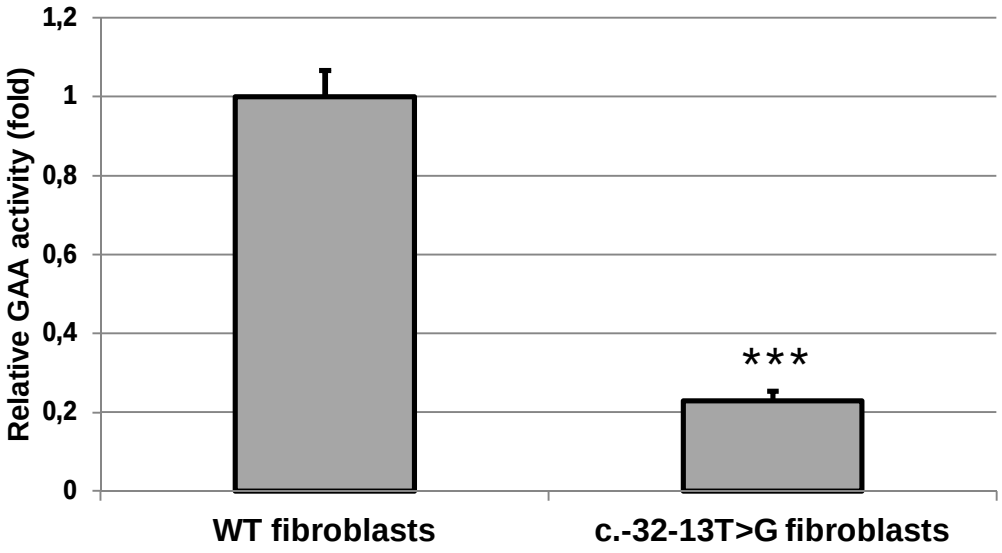
1,2
1
0,8
0,6
0,4
0,2
0
Relative GAA activity (fold)
***
WT fibroblasts
c.-32-13T>G fibroblasts

b

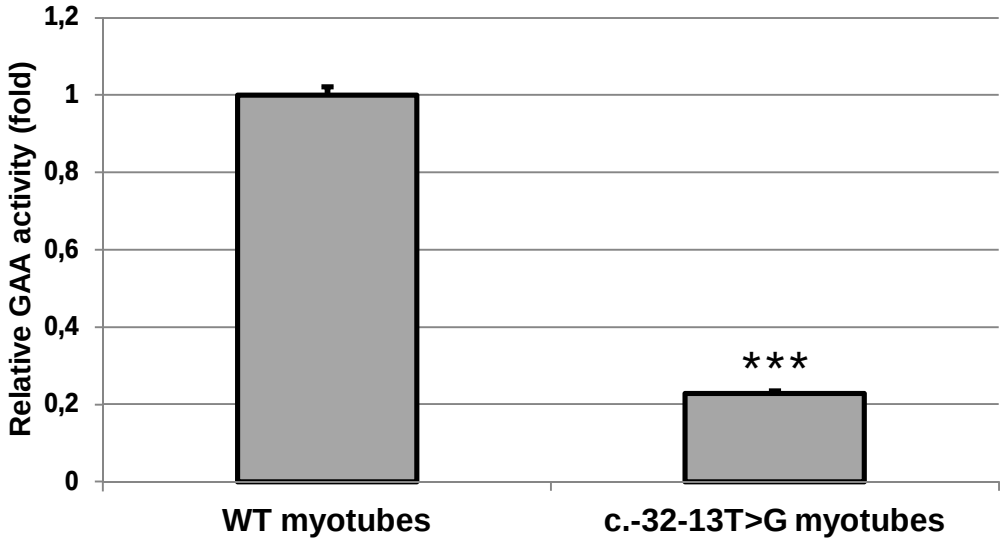
1,2
1
0,8
0,6
0,4
0,2
0
Relative GAA activity (fold)
***
WT myotubes
c.-32-13T>G myotubes

Figure S7.

a

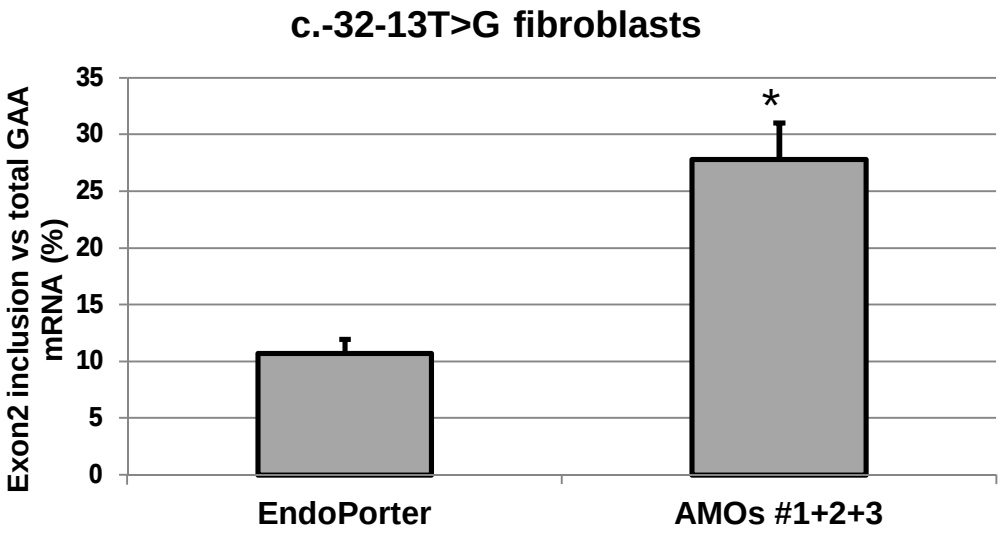
c.-32-13T>G fibroblasts
Exon2 inclusion vs total GAA mRNA (%)
35
30
25
20
15
10
5
0
*
EndoPorter
AMOs #1+2+3

b

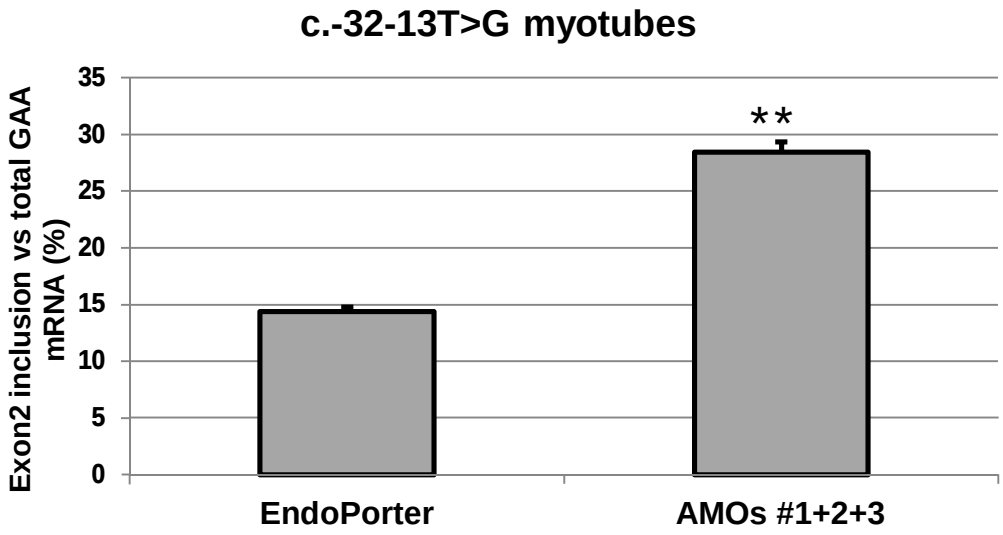
c.-32-13T>G myotubes
Exon2 inclusion vs total GAA mRNA (%)
35
30
25
20
15
10
5
0
**
EndoPorter
AMOs #1+2+3

Figure S8.

a

LO-GSDII myoblasts

Genotype: c.-32-13T>G; c.2646_2646+1delTG

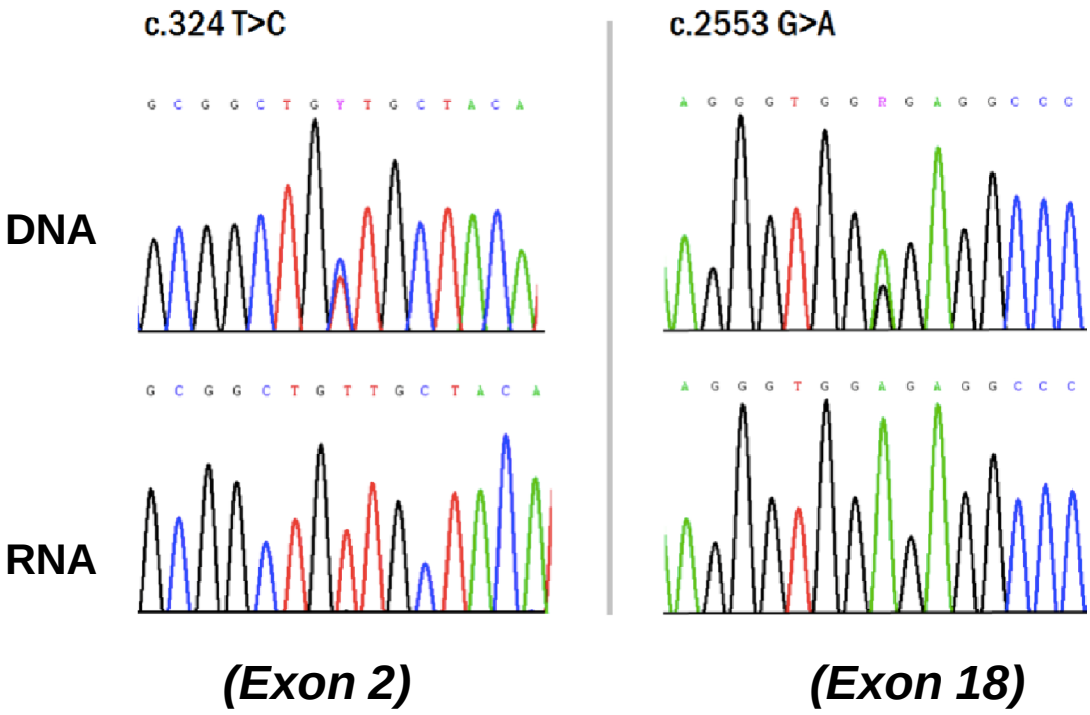

SUPPLEMENTARY FIGURE LEGENDS.

Supplementary Figure 1. Quantification of *GAA* exon 2 inclusion in HeLa transfected with *GAA* delta exon 2 MUT and WT minigenes. (a-b) Graphical representation of the quantification of the intensity of the bands corresponding to the *GAA* exon 2 (N) generated after transfection of GAA delta exon 2 MUT and WT minigenes. The intensity of the bands analyzed by ImageJ and expressed as a percentage. Data are represented as means ± SD of three independent experiments (***$P< 0.001$). **(c)** Schematic illustration of the Δ357-500 minigene and the position of the new activated cryptic 3'ss. The new 3'ss is located 91nt upstream the Δ357-500 region. The identity of the band was confirmed by sequencing.

Supplementary Figure 2. Screening of SFRS proteins able to bind *GAA* exon 2 by Western Blot analysis. (a) Western blot analysis after pull down assay using specific antibodies against SFRSs. The nuclear extract sample (NE) corresponds to 1/20th of the total amount of protein used for the pull down assay. The western blot pictures shows representative results of three independent experiments. Empty beads were used as a control (Beads). **(b-d)** Analysis performed by the bioinformatic tool SpliceAid2. Graphical representation of the putative binding sites for splicing factors within the 147-286nt (b), to 357-500nt (c) and to 427-572nt (d) regions of *GAA* exon 2. Positive scores were assigned to target sequences classified as exonic splicing enhancer motifs whereas negative scores to exonic splicing silencer motifs. The height and the width of the bars correlate with the binding affinity and the number of nucleotides encompassing the binding site, respectively. The splicing factor name predicted to bind each sequence is indicated on top of each bar.

Supplementary Figure 3. Analysis performed using the bioinformatic tool Human Splicing Finder 3. (a-c) Graphical representation of putative exonic regulatory regions within the 147-286nt (a), to 357-500nt (b) and to 427-572nt (c) *GAA* exon 2 sequences. The position of exonic splicing enhancer motifs is showed in the upper part of each graph whereas exonic splicing silencer motifs are reported in the lower part. (d) Each colour corresponds to a different prediction algorithm as

described in the panel d.

Supplementary Figure 4. Control AMO transfection does not affect splicing pattern of *GAA* ex2 MUT minigene. (a) RT-PCR analysis of HeLa cells co-transfected with AMOs #1,2 and 3 to a final concentration of 15 μM and the *GAA* ex2 MUT minigene. Control AMO was delivered to a final concentration of 10 μM together with the *GAA* ex2 MUT minigene. Cells transfected with the MUT minigene together with EndoPorter reagent and MUT minigene alone were used as internal control; not transfected cells (N.T.) were used as RT-PCR control. The agarose gel picture shows a representative result of three independent experiments. **(b)** Fluorescence distribution to confirm control AMO delivery. Brightfield and flurescence images at 20X and 40X magnification show the uptake of the control AMO fluorescently labeled in HeLa cells 48h after transfection. Cells show normal morphology and diffuse fluorescence distribution.

Supplementary Figure 5. Effect of AMOs against region 357-500 on exon 2 inclusion in the MUT minigene context. (a) Schematic representation of AMOs #5, 6 and 7 targeting the 357-500 region of *GAA* exon 2. The AMOs target sequences are indicated by black lines. **(b)** RT-PCR analysis of HeLa cells co-transfecetd with AMOs #5,6 and 7 and the *GAA* ex2 MUT minigene. AMOs were delivered as single unit or in different combination to a final concentration of 15 μM. Cells transfected with the mutated minigene together with EndoPorter reagent were used as internal control; not transfected cells (N.T.) were used as RT-PCR control. The agarose gel picture shows a representative result of three independent experiments. **(c)** RT-qPCR analysis of *GAA* exon 2 inclusion (N) in cells co-transfected with AMOs (#5+6+7) and the *GAA* MUT minigene. The relative abundance of N form is expressed as fold of increase over the *GAA* ex2 MUT minigene alone. RT-qPCR data are represented as means ± SEM of three independent experiments in a histogram plot (*P< 0.05; **P< 0.01; ***P< 0.001).

Supplementary Figure 6. GAA enzymatic activity in cultured fibroblasts and myotubes. GAA enzymatic activity in cultured fibroblasts (a) and myotubes (b) from a normal control (WT) and a

patient carrying the c.-32-13T>G mutation. Data are expressed as percentage of WT activity and represent the mean ± SEM of three independent experiments (*** = p<0,001; t-test statistics).

Supplementary Figure 7. Effect of AMOs targeting the 147-286 region on absolute percentage of exon 2 inclusion in patient's cells.

Exon 2 inclusion expressed as percentage of total *GAA* mRNA in c-32-13T>G fibroblasts (a) and myotubes (b) before and after 48h treatment with AMOs 1+2+3. The amount of exon 2 inclusion (N form) was analyzed using primers that specifically amplified mRNA containing exon 2 while the total amount of GAA transcript was determined using primers that target a region spanning *GAA* exon 18-19. Data are expressed as mean ± SEM of at least two independent experiments (* = p<0,05; ** = p<0,01; t-test statistics).

Supplementary Figure 8. Genomic DNA and mRNA Sanger sequencing of LO-GSDII myoblasts carrying the c.-32-13T>G and the c.2646_2646+1delTG mutations in the *GAA* gene.

(a) Electropherogram results showing two single nucleotide polimorfisms (c.324T>C in exon 2 and c.2553G>A in exon 18) that were found at the DNA but not at the mRNA level, indicating that only one *GAA* allele was expressed in these LO-GSDII myoblasts.

Table S1.

Primers for inserting deletions in pTB GAA Wt and MUT minigenes:

Δ7-146Fw	5'-tgagcccgctttcttctcccgcagGCCTGTCCCCGAGAGCTGAGTGGCTCCTC CCCAGTC-3'
Δ7-146Rv	5'-GACTGGGGAGGAGCCACTCAGCTCTCGGGGACAGGCctgcgggagaa gcaagcgggctca-3'
Δ77-216Fw	5'-CCCGCCCTGCTCCCACCGGCTCCTGGCCGTGACCAGGGCCCCGG GATGCCCAGGCACACC-3'
Δ77-216Rv	5'-GGTGTGCCTGGGCATCCCGGGGCCCTGGTCACGGCCAGGAGCCG GTGGGAGCAGGGCGGG-3'
Δ147-286Fw	5'-ACATCCTACTCCATGATTTCCTGCTGGTTCCCCAACAGCCGCTTCG ATTGCGCCCCTG-3'
Δ147-286Rv	5'-CAGGGGCGCAATCGAAGCGGCTGTTGGGGAACCAGCAGGAAATC ATGGAGTAGGATGT-3'
Δ217-356Fw	5'-CTCACCCAGCTCACCAGCAGGGAGCCAGCATGCTACATCCCTGCA AAGCAGGGGCTGCAG-3'
Δ217-356Rw	5'-CTGCAGCCCCTGCTTTGCAGGGATGTAGCATGCTGGCTCCCTGCT GGTGAGCTGGGTGAG-3'
Δ287-426Fw	5'-CAGAGCAGTGCCCACACAGTGCGACGTCCCGCTACCCCAGCTACA AGCTGGAGAACCTGA-3'
Δ287-426Rw	5'-TCAGGTTCTCCAGCTTGTAGCTGGGGTAGCGGGACGTCGCACTGT GTGGGCACTGCTCTG-3'
Δ357-500Fw	5'-ACCCAGGAACAGTGCGAGGCCCGCGGCTGTCCCACCTTCTTCCCC AAGGACATCCTGACC-3'
Δ357-500Rw	5'-GGTCAGGATGTCCTTGGGGAAGAAGGTGGGACAGCCGCGGGCCT CGCACTGTTCCTGGGT-3'
Δ427-572Fw	5'-TGGGGCAGCCCTGGTGCTTCTTCCCACCCATTCACGgtgggcagggcag gggcgggggcg-3'
Δ427-572Rv	5'-cgcccccgcccctgccctgcccacCGTGAATGGGTGGGAAGAAGCACCAGG GCTGCCCCA-3'

Primer for inserting the single mutation -13T/G:

hGAA-13Gs	5'-GAGCCCGCTTGCTTCTCCCGC-3'
hGAA-13Gas	5'-GCGGGAGAAGCAAGCGGGCTC-3'

Primer for end-point PCR on GAA cDNA after AMOs treatment:

GAA Fw	5'-CCACCTCTAGGTTCTCCTCGT-3'
SKIP2 Rv	5'-CGGAGAACTCCACGCTGTA-3'

Primers for RT-PCR:

GLO 800Bis Rv	5’-CACAGAAG**C**CAG**G**AACTTGTCC-3’
Alfa 2-3 Fw	5’-CAACTTCAAGCTCCTAAGCCACTGC-3’
BRA 2 Rv	5’-TAGGATCCGGTCACCAGGAAGTTGGTTAAATCA-3’

Oligo morpholino:

Oligo #1 (199-223)	5’-CCTGGTCTGCTGGCTCCCTGCTGGT-3’
Oligo #2 (230-254)*	5’-ACGaCCGGGGTGTGCCTGaGCATCC-3’
Oligo #3 (258-282)	5’-CGTCGCACTGTGTGGGCACTGCTCT-3’
Oligo #5 (394-418)	5’-AAGAAGCACCAGGGCTGCCCCATCT-3’
Oligo #6 (435-459)	5’-AGCTCAGGTTCTCCAGCTTGTAGCT-3’
Oligo #7 (456-480)	5’-CCGTGTAGCCCATTTCAGAGGAGCT-3’

*Morpholino #2 (230-254) carries two point mutation (underlined letters) to avoid strong secondary structure, without compromising its binding to the target sequence.

Primers for RealTime PCR:

GAA F3 Fw	5’-CCCGGCCTGGAGTACAATG-3’
GAA R3 Rv	5’-CAGGAGTGCAGCGGTTGC-3’
AlfaGlo2 142 Fw	5’-ACCAAGACCTACTTCCCGCACTTCG-3’
AlfaGlo2-3 294 Rv	5’-CAGGCAGTGGCTTAGGAGCTTGAAG-3’
GAA ex1-2 Fw	5’-CCACCTCTAGGTTCTCCTCGT-3’
GAA ex1-2 Rv	5’-TCCTACAGGCCCGCTCC-3’
GAA ex18-19 Fw	5’-GAGCTGTTCTGGGACGATG-3’
GAA ex18-19 Rv	5’-GCAGCTGCAGGCCAGCTCC-3’
HPRT Fw	5’-GACCAGTCAACAGGGGACAT-3’
HPRT Rv	5’-GTGTCAATTATATCTTCCACAATCAAG-3’

Primers for Pulldown:

T7 147-286 Fw	5’-TAATACGACTCACTATAGGGCCCCGAGAGCTGAGTGGCTC-3’
147-286 Rv	5’-GGGACGTCGCACTGTGTGGGCAC-3’
T7 357-500 Fw	5’-TAATACGACTCACTATAGGGTGCTACATCCCTGCAAAGCA-3’
357-500 Rv	5’-GGTGGTACGGGTCAGGGTGGCCGTG-3’
T7 427-571 Fw	5’-TAATACGACTCACTATAGGGGCTACCCCAGCTACAAGCTG-3’
427-571 Rv	5’-TGGAGGCGGTTCTCAGTCTCCATC-3’

Table S2. Normality test (Shapiro-Wilk). *p*-values >0.05 indicate a normal distribution.

HeLa cells co-transfected with AMOs #1, 2 and 3 and the *GAA* MUT minigene (Fig. 3c).

Dataset	W	n	*p*-values
Endoporter	0.938340	10	0.534700
AMO #1	0.824235	8	0.051689
AMO #2	0.994243	4	0.978066
AMO #3	0.839796	4	0.194808
AMO #1+2	0.769482	4	0.057806
AMO #1+3	0.918227	4	0.527055
AMO #2+3	0.788121	4	0.082567
AMO #1+2+3	0.943869	6	0.690506

HeLa cells co-transfected with AMOs #5, 6 and 7 and the *GAA* MUT minigene (Fig. S5c).

Dataset	W	n	*p*-values
Endoporter	0.946550	9	0.652269
AMO #5	0.897723	5	0.397426
AMO #6	0.773414	3	0.052494
AMO #7	0.855847	3	0.256216
AMO # 5+6	0.855684	5	0.213163
AMO # 5+7	0.772879	3	0.051274
AMO # 6+7	0.830194	3	0.188826
AMO # 5+6+7	0.927684	7	0.531376

Patient fibroblasts transfected with AMOs #1, 2 and 3 (Fig. 4b).

Dataset	W	n	*p*-values
Endoporter	0.854651	3	0.252970
AMO #1	0.779125	3	0.065581
AMO #2	0.919708	3	0.451310
AMO #3	0.979908	3	0.728367
AMO #1+2+3	0.935960	3	0.511376